Vulnerability to extreme drought is linked to hydraulic strategies and not carbohydrate use across 12 rainforest tree species

Camille Ziegler[1,2]* (ORCID: 0000-0002-0855-1347), Hervé Cochard[3] (ORCID: 0000-0002-2727-7072), Clément Stahl[1] (ORCID: 0000-0001-5411-1169), Louis Foltzer[2], Bastien Gérard[2] (ORCID: 0000-0003-3132-05), Jean-Yves Goret[1] (ORCID: 0000-0003-3604-5756), Patrick Heuret[1,4] (ORCID: 0000-0002-7956-0451), Sébastien Levionnois[1,4] (ORCID: 0000-0002-7217-9762), Pascale Maillard[2] (ORCID: 0000-0002-6088-8561), Damien Bonal[2†] (ORCID: 0001-9602-8603), Sabrina Coste[1†] (ORCID: 0000-0003-3948-4375)

[1]UMR EcoFoG, AgroParisTech, CIRAD, CNRS, INRAE, Université des Antilles, Université de Guyane, 97310 Kourou, France.
[2]Université de Lorraine, AgroParisTech, INRAE, UMR SILVA, 54000 Nancy, France.
[3] Université Clermont-Auvergne, INRAE, PIAF, 63000 Clermont-Ferrand, France
[4]AMAP, Univ. Montpellier, CIRAD, CNRS, INRAE, IRD, 34000 Montpellier, France.

*Author for correspondence:
Camille Ziegler, PhD
Email: camille.ziegler9@gmail.com
[†]Joint Senior authors. D.B and S.C. contributed equally to this work.

SUMMARY

- Knowledge on the physiological mechanisms underlying species vulnerability to drought is critical to better understand tree mortality patterns. Investigating the diversity of plant adaptive strategies to drought is therefore timely, especially in tropical rainforest species.
- We investigated whether hydraulic strategies determined the ability of saplings to use stored non-structural carbohydrates during an extreme imposed drought in a controlled experiment on 12 rainforest tree species. We further explored drought-survival mechanisms with a modeling approach.
- Hydraulic strategies varied considerably across species with a trade-off between dehydration-tolerance and -avoidance. Independently to hydraulic strategies, whole-plant starch concentrations strongly declined during drought in most species, allowing a maintenance or an increase in soluble sugar concentrations, accompanied by elevated stem xylem embolism levels (>70%). Modeled time to hydraulic failure (THF) varied considerably across species and was related to residual water conductance.
- Carbon starvation was widespread, yet our data indicate that hydraulic failure was the prevailing mortality process in the studied species, regardless of the contrasting hydraulic strategies they exhibited. Dehydration-avoidance nevertheless seems to be an effective drought-survival strategy at the sapling stage. Further investigations on residual water losses may be key to understanding the response of tropical rainforest tree communities to climate change.

Keywords: drought-induced mortality, hydraulic failure, hydraulic strategies, minimum conductance, nonstructural carbohydrates (NSC), SurEau model, tropical forests, xylem embolism

INTRODUCTION

Recent drought episodes have been shown to cause widespread tree mortality across biomes (Brodribb *et al.,* 2020; Hartmann *et al.,* 2022) and tropical rainforests have not been spared (Phillips *et al.,* 2009, 2010; Powers *et al.,* 2020; Browne *et al.,* 2021). Main uncertainties in global vegetation models predicting future tropical rainforests dynamics are related to their physiological response to climate (Huntingford *et al.,* 2013). This is why gaining more in-depth knowledge on the coordination among the main physiological mechanisms underlying species drought-survival is a major challenge (McDowell *et al.,* 2022). Particular concern is given to saplings which represent the future of these forests and are under strong selective pressure due to drought, with yet a lack of a mechanistic understanding causing the observed floristic shifts over Amazonia (Esquivel-Muelbert *et al.,* 2019).

Plant adaptive strategies to drought are expressed as a simultaneous and sequential combination of multiple traits, which vary substantially across species (Pivovaroff *et al.,* 2016; Choat *et al.,* 2018; Volaire, 2018). This is especially true in hyper-diverse tropical rainforests exhibiting strong functional diversity (Oliveira *et al.,* 2021). Strong declines in tree water potential cause irreversible loss in stem xylem hydraulic conductivity (i.e. *runaway embolism*) and death as a result of hydraulic failure limiting the water supply to living tissues (Tyree & Sperry 1988; Mantova *et al.,* 2021, 2022; McDowell *et al.,* 2022). Hydraulic strategies are commonly characterized by mechanisms allowing plants to delay time to hydraulic failure (THF) by either tolerating low tissue-level hydration and/or to minimizing water losses, i.e. dehydration-tolerance and avoidance (Volaire, 2018).

Stem xylem vulnerability to embolism, quantified as the water potential causing 50% loss in xylem hydraulic conductivity ($P_{50,stem}$), is a central trait involved in dehydration-tolerance and is linked to drought-survival (Urli *et al.,* 2013; Anderegg *et al.,* 2015, 2016) and the ability to thrive in dry environments (Larter *et al.,* 2017; Oliveira *et al.,* 2019). Embolism tolerance, defined as the amount of stem xylem embolism plants can tolerate without dying, may however vary substantially across species (Brodribb *et al.,* 2010; Urli *et al.,* 2013; Li *et al.,* 2016; Adams *et al.,* 2017; Hammond *et al.,* 2019; Shao *et al.,* 2022).

Several mechanisms are involved in dehydration-avoidance. Plants can avoid losing water through stomatal closure, quantified as the water potential causing 90% loss in maximum stomatal conductance ($P_{closure}$). Delaying stomatal closure may allow sustained carbon assimilation, yet timely stomatal closure allows a drastic reduction in water losses and the further decrease of tree water potentials (Martin St-Paul *et al.,* 2017; Creek *et al.,* 2020). If soil water availability is not replenished, water continues to be lost by residual vapor fluxes through leaf cuticles and leaky stomata, i.e. minimum leaf conductance (g_{min}; Duursma *et al.,* 2019), as well as through bark cuticles and lenticels, i.e. bark conductance (g_{bark}; Loram-Lourenço *et al.,* 2022; Rosner & Morris, 2022). Thus, species with broad

stem stomatal safety margins, i.e. reaching $P_{closure}$ long before $P_{50,stem}$, as well as with low values of g_{min} and g_{bark}, may delay THF (Martin St-Paul *et al.,* 2017; Duursma *et al.,* 2019; Machado *et al.,* 2020; Wolfe, 2020; Levionnois *et al.,* 2021a; Loram-Lourenço *et al.,* 2022). Moreover, it has been evidenced that species showing vulnerability segmentation, i.e. with leaf xylem being more vulnerable to embolism than stem xylem, may also delay THF (Blackman *et al.,* 2019b; Levionnois *et al.,* 2021a). The aforementioned traits may vary considerably across coexisting rainforest tree species (Ziegler *et al.,* 2019; Levionnois *et al.,* 2020; Levionnois *et al.,* 2021a; Slot *et al.,* 2021) but much remains to be explored on how they shape species' hydraulic strategies or how these traits influence specie's drought-survival (Blackman *et al.,* 2019ab; Li *et al.,* 2019).

The risk of drought-induced mortality has been conceptualized in a framework describing the linkage between water and carbon depletion and declines in their fluxes relative to demand by living tissues (McDowell *et al.,* 2008, 2011, 2022). Hydraulic failure has been shown to be a relatively ubiquitous process preceding drought-induced mortality (Adams *et al.,* 2017). Yet it may be interrelated with carbon starvation, the process by which a limited supply of non-structural carbohydrates (NSC) impairs the maintenance of carbon-dependent metabolic, defense or hydraulic functions (McDowell *et al.,* 2022). As a corollary of the tight linkage between transpiration and photosynthetic assimilation, stomatal closure causes a cessation of carbon gain (Taiz & Zeiger, 2002). This constrains plants to remobilize starch into soluble sugars to be able to maintain diverse functions necessary for survival such as osmoregulation and cell respiration (Mitchell *et al.,* 2013; Hartmann & Trumbore, 2016). For instance, the loss of adequate soluble sugar concentration required for osmoregulation can promote the failure to maintain hydraulic integrity and is therefore a potential trigger of hydraulic failure (Sevanto *et al.,* 2014). In seedlings of rainforest tree species, individuals with higher pre-drought NSC concentrations better maintained water potentials and survived longer during drought (O'Brien *et al.,* 2014). This was probably due to a better maintenance of osmotic potentials and water transport capacity. Yet, to date, the potential interplay between the use of NSC and the loss of xylem hydraulic conductance has mainly been studied for temperate species (see the meta-analysis by Adams *et al.,* 2017), which urges to consider this matter in tropical species.

In this study, we investigated the hydraulic and carbon response of saplings belonging to 12 common rainforest tree species to an extreme drought, by combining experimental and modeling approaches in order to:

(i) characterize the diversity of hydraulic strategies of coexisting rainforest tree species,

(ii) evaluate if species hydraulic strategies determine the prevalence of non-structural carbohydrate depletion during drought-induced hydraulic failure,

(iii) identify the hydraulic strategies underlying specie's vulnerability to drought during an extreme simulated drought.

For (i), we specifically addressed the interspecific variability in traits shaping hydraulic strategies as well as the potential coordination or compromises among these traits. For (ii), we tested the ability of species to use stored NSC during an extreme drought to compensate for a lack of carbon assimilation. For (iii), we evaluated the effects of hydraulic and NSC-use traits on time to hydraulic failure by using the mechanistic model *SurEau*. This allowed to test whether particular trait syndromes would be advantaged or disadvantaged in a context of increasing drought intensity and duration.

MATERIALS AND METHODS

Species and growing conditions

We studied saplings of 12 tree species naturally occurring tropical rainforests (Table 1; Fig. S1). Seeds or seedlings of 11 species originated from Paracou (5°16′26″N, 52°55′26″W), a lowland tropical rainforest about 60 km from Kourou, French Guiana. One species, *E. coriacea*, was collected at the Bafog site in western French Guiana (5°36′36″N, 53°52′48″W). Out of the 12 selected species, 11 naturally occur in French Guiana in habitats with contrasting soil water availability (Allié *et al.,* 2015) and were selected according to known or putative differences in their vulnerability to drought (Baraloto *et al.,* 2006, 2007; Fortunel *et al.,* 2014; Maréchaux *et al.,* 2015; Fargeon *et al.,* 2016). One of these species, *H. utilis*, originates from relatively mesic habitats in West Africa (Bongers *et al.,* 1999) and is experimentally planted in French Guiana.

Seeds or seedlings (< 1 year old) were collected in the near vicinity of at least three different adult trees per species between May 2016 and March 2017. Seeds were sown and seedlings planted in 4-liter pots containing a 2:1 (v/v) mixture of brown forest ferralitic clay soil and sand. Plants grew under ca. 7% of total irradiance and were drip-irrigated three times a day. After 10 to 24 months in these conditions, ca. 90 saplings per species were selected and repotted into 19-liter pots (25 x 40 cm) containing the same substrate. They then grew at 19 ± 0% of total irradiance and were watered manually three times a week during 3 months before the start of the experimental manipulation of soil water availability. During this period, saplings were fertilized twice with a slow-release fertilizer (Jarditropic 12:12:17). Light, air temperature and relative air humidity were monitored continuously at 30 min intervals using Environmental HOBO sensors (Amanvillers, France). Mean (± SE) day and night air temperature was 30.7 ± 0.1 °C and 26.7 ± 0.0 °C, respectively, with an average 4.0 °C difference between the dry and the rainy season. Mean (± SE) day and night relative air humidity was 71.8 ± 0.3% and 85.7 ± 0.2%, respectively, with an average 13.9% difference between seasons.

Experimental setup

The drought experiment took place in a shadehouse at the Campus Agronomique of Kourou, French Guiana, between June 2017 and March 2019. For practical reasons, it was divided into three consecutive cycles, each containing four species (Table 1). At the start of the experiment, saplings were 18-29 months old. For each species, a total of 48 saplings were randomly assigned to either a well-watered or a drought treatment (Fig. S2). Plants were harvested when droughted saplings reached a severely wilted stage (Tyree *et al.,* 2002; Tyree *et al.,* 2003; Engelbrecht *et al.,* 2007b; Kursar *et al.,* 2009, Manzi *et al.,* 2022). At harvest, leaf water potentials and NSC concentrations were measured in both treatments. Additional well-watered plants were used to determine leaf and stem xylem

vulnerability to embolism, as well as additional severely wilted plants to refine estimations of lethal plant water potential (see details of trait measurements below).

Gas exchange and leaf water potential

Stomatal conductance for water vapor (g_s; mmol m^{-2} s^{-1}) was measured on several occasions on clear days between 8:00 and 11:00 am, on the abaxial side of one fully expanded newly mature leaf per sapling on 10 well-watered saplings per treatment using a porometer (AP4; Delta T Devices, Ltd, Cambridge, UK). Maximum stomatal conductance ($g_{s,max}$) was determined by averaging the 10 highest values of g_s. Leaf water potential (P_{md}; MPa) was recorded at harvest between 11:00 and 15:00 with a pressure chamber (1505D-EXP, PMS Instrument Co., Albany, OR, USA), on 3 leaves per plant on 14-23 well-watered plants and 10-30 severely wilted plants per species.

Leaf water potential at turgor loss point

The water potential at stomatal closure ($P_{closure}$) has been shown to be mechanistically related to changes in turgor or volume of neighboring cells (Rodriguez-Dominguez *et al.,* 2016; Buckley, 2019). For this reason, $P_{closure}$ is commonly estimated using leaf turgor loss point (P_{tlp}; Martin-StPaul *et al.,* 2017). We measured P_{tlp} on 10 well-watered plants per species using a vapor pressure osmometer (VAPRO 5520, Wescor, Logan, UT, USA; Bartlett *et al.,* 2012). One leaf per plant was harvested in the early morning, immediately placed in a sealed plastic bag containing moist absorbent paper, placed in a cooler, and taken back to the neighboring laboratory to be placed at 5°C for overnight rehydration. The following day, P_{tlp} was measured according to Bartlett *et al.,* (2012). Whether or not well-watered plants closed stomata at midday was calculated as the differences between P_{md} and P_{tlp}.

Minimum leaf conductance

The minimum leaf conductance (g_{min}, mmol m^{-2} s^{-1}) was measured from leaf drying curves on 10 well-watered plants per species following the detailed protocol described in Sack and Scoffoni (2011), using a precision balance (AB 204-S, Mettler Toledo). One leaf per plant was harvested in the early morning. g_{min} was calculated as the slope of the linear part of the leaf drying curves reflecting the rate of leaf water loss after stomatal closure, divided by VPD and normalized by leaf size (i.e. 2 x LS; cm^2). For species with compound leaves, a leaflet was used.

Stem xylem vulnerability to embolism

Stem xylem hydraulic vulnerability to embolism was characterized using the bench dehydration technique (Sperry *et al.,* 1988) on a total of 11 to 31 well-watered plants per species. Plants were

dehydrated at a constant air temperature of 25°C to reach a broad range of water potentials and bagged for at least 12 hours to allow water potential equilibrium. Then, for each plant, a 5 cm long and 3-5 mm wide stem segment was cut and used to measure stem xylem hydraulic conductivity. The stem xylem water potential was estimated from the leaf water potential measured with a pressure chamber on 3-5 leaves per plant situated on or adjacent to the stem segment. The stem segment was shaved at both ends under water and connected to a xylem embolism meter mounted with a digital liquid flow meter (XYL'EM and LiquiFlow L13, Bronkhorst Instrutec, Montigny-les-Cormeilles, France). For each individual plant, native stem hydraulic conductivity was measured using a filtered (0.2 µm) and degassed solution of 10 mM KCl and 0.1 mM $CaCl_2$. Any embolism was then removed by repeatedly flushing the stem at a constant pressure of 200 KPa and maximum stem conductivity was recorded. The percentage loss in stem xylem hydraulic conductivity (PLC) was then calculated as the relative difference in flow before and after flushing and plotted against water potential, known as the vulnerability curve. One species, *S. pruriens*, was recalcitrant to the method.

Leaf xylem vulnerability to embolism

Leaf xylem hydraulic vulnerability to drought-induced embolism was characterized using the optical visualization method (Brodribb *et al.,* 2016) on 2-3 well-watered plants per species. For a complete description of the method, see Brodribb *et al.* (2016). Plants were dehydrated at a constant air temperature of 25°C while embolism events were detected and quantified using a high spatial resolution scanner (6400 dpi; Epson Perfection V800; Epson America Inc., Long Beach, CA, USA) and a customized ImageJ macro (https://imagej.nih.gov/ij/). Plant water potential was measured continuously using an automated stem psychrometer (PSY1; ICT International, Armidale, NSW, Australia) installed on the stem and close to the imaged leaf assuming that leaf and stem water potentials are near-equilibrium in non-transpiring shoots (Meinzer *et al.,* 2016). The linear evolution of plant water potential was recorded every 20 min with the ICT Instrument Device Chooser software. By combining it to the evolution of the percentage of 'embolized pixels' over time, vulnerability curves were constructed. For some species, embolism events could not be observed in thick and lignified midribs. Therefore, only embolism events occurring in second, third and higher vein orders were considered to allow cross-species comparison. Two species, *H. utilis* and *J. copaia*, were recalcitrant to the method.

Vulnerability curve fitting, stomatal safety margins and vulnerability segmentation

For each species, vulnerability curves were fitted using a sigmoidal function (Pammenter & Van der Willigen, 1998) using the '*fitplc'* function of the *fitPLC* package in R (Duursma & Choat 2017).

Parameters describing xylem vulnerability to embolism were extracted from the curve fitting, such as $P_{50,leaf}$, the water potential associated with 50% of 'embolized pixels' and $P_{50,stem}$ and $P_{88,stem}$, the water potentials (MPa) associated with 50 and 88% loss in stem hydraulic conductivity. Bootstrap 95% confidence intervals (CIs) were calculated. Stomatal hydraulic safety margins were estimated at the leaf (SSM_{leaf}) and stem level (SSM_{stem}) as the difference between P_{tlp} and $P_{50,leaf}$ or $P_{50,stem}$, respectively. The degree of vulnerability segmentation was calculated as the difference between $P_{50,leaf}$ and $P_{50,stem}$ (Seg_{P50}). Species were considered positively segmented when the CIs around mean values of $P_{50,leaf}$ and $P_{50,stem}$ did not overlap (Duursma & Choat 2017). The measurements of leaf and stem xylem vulnerability to embolism were made with two different methods which have shown to produce similar estimates (Brodribb *et al.,* 2016, 2017). All traits were analyzed using species means.

Lethal water potential and percent loss in hydraulic conductance

The water potential associated with 50% mortality of saplings (i.e. lethal water potential; P_{lethal}; MPa) was estimated from leaf water potentials of severely wilted plants ($P_{md,SW}$; MPa) using a previously established equation from Kursar *et al.,* (2009), such as $P_{lethal} = 1.11 \times P_{md,SW}$ ($R^2 = 0.68$; $p < 0.0001$; $n = 20$). Vulnerability curves and $P_{md,SW}$ or P_{lethal} were used to estimate the percent loss of leaf and stem xylem hydraulic conductance of severely wilted plants ($PLC_{SW,leaf}$ and $PLC_{SW,stem}$, %) and to determine the PLC threshold of leaves and stems for survival ($PLC_{leth,leaf}$ and $PLC_{leth,stem}$, %).

Non-structural carbohydrates

Non-structural carbohydrates (NSC) were measured on leaves, stems and roots of 7 saplings per species and per treatment at the end of the experiment. Two to five evenly distributed leaves, basal and distal stem segments and a subsample of coarse and fine roots were cut and immediately frozen in liquid N for at least 10 min. They were stored at -18°C then freeze-dried at -50°C for 48h and ground to fine powder using a ball mill (Mixer Mill MM301, Retsch, Germany). Total SS concentration was determined by the anthrone-sulfuric acid colorimetric method following Van Handel, (1965) at 620 nm (spectrophotometer UV-visible DU 640 B, Beckman Coulter, USA). Starch concentration was determined colorimetrically at 530 nm using an enzymatic method. Methods are detailed in Svensk et al. (2020). SS and starch contents were expressed as percent DM (Dry Mass) for each organ of each individual plant. Whole plant NSC concentrations were calculated according to O'Brien *et al.,* (2014). The response in SS and starch concentrations in droughted compared to well-watered plants was then calculated for each NSC type in leaves, stems, roots and whole plant (varSS, varStarch; %) as a normalized deviation from the difference between individual concentration values of severely wilted plants and mean species value of well-watered plants. To investigate the relative importance of

physiological drought-induced mortality processes, NSC deviation from control was compared to leaf and stem PLC values estimated on the same individuals (n = 7). To estimate the amount of NSC used during drought, the concentration in NSC of droughted plants was subtracted to the concentration of well-watered plants (ΔSS and ΔStarch; % DM).

Growth and biomass data

Stem height and basal diameter were recorded at the beginning and at the end of the experiment for all plants with a tape measure and a digital caliper (Digimatic micrometer, Mitutuyo, Japan), respectively. Relative growth rate in stem volume (RGR; $cm^3\ y^{-1}$) was calculated assuming a constant tapering of the stem. At harvest, leaf, stem and root dry biomass were recorded for each plant after drying at 60°C for 72h. Leaf area of well-watered plants (A_l; cm^2) was estimated by multiplying total leaf dry mass by LMA. The ratio of leaf area to sapwood area (A_l:A_s) was then estimated by dividing A_l by basal stem area.

Data analyses

All analyses were performed with the R software. To determine the diversity of drought-survival strategies and visualize potential trait correlations, we ran a principal component analysis (PCA) with the *FactoMineR* and *factoextra* packages. Some traits - i.e. SSM_{leaf}, SSM_{stem}, Seg_{P50}, THF - were added as supplementary quantitative variables because they were directly computed from, and strongly autocorrelated to other traits and would have introduced bias. Bivariate trait correlations were explored using simple linear regressions or standardized major axis regression (Warton *et al.,* 2006) with the *smatr* package (Falster *et al.,* 2006) when there was no *a priori* on the causality of the relationship between traits. Relationships were summarized in a Pearson correlation matrix using the *corrplot* package (Fig. S3). Values of $P_{50,leaf}$ were gapfilled for *H. utilis* and *J. copaia*, and of $P_{50,stem}$ for *S. pruriens* by using the linear relationships between $P_{50,leaf}$ and wood density ($R^2 = 0.40$) and between $P_{50,stem}$ and g_{min} ($R^2 = 0.54$). Gapfilled values were used only for PCA, correlation matrix and in *SurEau*. When applicable, interspecific variability in the measured traits was tested with one-way ANOVA. To analyze the interspecific variability in the effects of drought on NSC use, we used a two-factor ANOVA, with '*Species'* and '*Treatment'* as factors. Differences in NSC concentrations across treatments for each species were tested using t-tests, Wilcoxon test or Welch t-test according to normality and heteroscedasticity of the data.

Simulations with the SurEau model

To evaluate the contribution of the different physiological traits to the drought resistance of the studied species, we used the process-based *SurEau* model (Cochard *et al.,* 2021). *SurEau* simulates THF by jointly considering stomatal and hydraulic traits, plant size, as well as climate and soil properties. The model was parameterized with species' trait data measured in this study. Stomatal closure occurred when the leaf water potential was equal to P_{tlp}. The formation and propagation of xylem embolism followed vulnerability curve parameters determined for leaves and stems. We assumed that the trunk and the roots had the same vulnerability than the branches. Area-based leaf residual water losses were estimated from g_{min} and leaf VPD values. Area-based bark residual conductance (g_{bark}) was estimated to be equal to g_{min} (Levionnois *et al.,* 2021a; Loram-Lourenço *et al.,* 2022). Internal water stores were estimated from stem volume based on interspecific variation of the leaf to stem area ratio (A_l:A_s). After stomatal closure, water losses were estimated from g_{min} and leaf area, and g_{bark} and bark area. The model parameters that were not measured were given realistic values according to the literature and considered constant across species. A more detailed description of the model parametrization can be found in the supplementary material (Table SX). We computed time to stem hydraulic failure ($THF_;$ days) as the time between complete stomatal closure and the moment when the stem reaches 99 % loss of hydraulic conductivity, causing irreversible hydraulic damage and subsequent death by hydraulic failure. This threshold guarantees that plant water pools were almost empty and that no other water reservoirs are available for the plant (Cochard *et al.,* 2021).

A first set of simulations was run using a mean estimated leaf area (A_l) per species. Species with larger A_l had shorter THF since A_l is a strong driver of water losses. Since it may be a confounding factor when predicting the kinetics of plant dehydration and desiccation (Lopez *et al.,* 2021), we ran a second set of simulations assuming species had a similar A_l, but specific values of A_l:A_s. Since we did not measure the water potential at stomatal closure directly from gas-exchange measurements, we also ran the model on the assumption that the point of stomatal closure corresponds to the formation of leaf xylem embolism, quantified as the water potential causing 12% of leaf xylem embolism ($P_{12,leaf}$). Values of simulated THF using either P_{tlp} or $P_{12,leaf}$ as an estimator of stomatal closure were strongly coordinated (Fig. S6). For data analysis, we further used THF simulated from P_{tlp} data. We then performed for each species a variance-based global sensitivity analysis to identify the hydraulic traits that influence THF. Variance-based approaches can measure sensitivity across the whole input space and quantify the effect of interactions that can be unnoticed on a local sensitivity analysis approach (i.e., when moving one parameter at a time). Here, we used the Sobol' sensitivity analysis method (Sobol, 2001) using the *sensobol* R package (Puy *et al.,* 2022), and reported 'Sobol's total order indices' that quantify the contribution of each parameter (i.e. hydraulic traits) to the variance of THF. For each

302 species, we ran 10,000 simulations while allowing each parameter to vary randomly within a range of
303 ±20% of the observed value.

RESULTS

Diversity of hydraulic strategies

All the investigated hydraulic traits varied significantly across species (see Table 2 for mean trait values and Fig. S3 for trait correlations). PCA revealed three primary axes of variation that cumulatively explained 81.7% of total variation (Fig. 1). Species were relatively evenly distributed according to the two first axes, revealing contrasting hydraulic strategies. The first axis (45% of total variation) discriminated species according to a trade-off between $P_{50,stem}$ and P_{lethal} on the one hand (Fig. S3), and g_{min} on the other hand. Species with the lowest values of g_{min} displayed less negative values of $P_{50,stem}$ (Fig. 2a) and P_{lethal}, and larger SSM_{stem} (Fig. S3). There was a positive relationship between P_{lethal}, $P_{50,stem}$ and $P_{88,stem}$ (Fig. 2b; Fig. S3). The second axis (23.8% of total variation) discriminated species according to A_l:A_s, $P_{50,leaf}$ and SSM_{leaf}. The third axis (12.9% of total variation) mostly discriminated species according to P_{tlp} and to a lesser extent according to g_{min}.

As a result of the relatively low interspecific variation in P_{tlp}, P_{tlp} was unrelated to $P_{50,leaf}$ and $P_{50,stem}$ (Fig. S3). There was no relationship between $P_{50,leaf}$ and $P_{50,stem}$ (Fig. S3). $SegP_{50}$ was positive for five out of the nine studied species for which $P_{50,leaf}$ and $P_{50,stem}$ data were available. Higher values of $SegP_{50}$ were promoted by less negative values of $P_{50,leaf}$ and more negative values of $P_{50,stem}$ (Fig. 2c). There was a positive relationship between $SegP_{50}$ and SSM_{stem} and a trade-off between $SegP_{50}$ and SSM_{leaf} (Fig. 2d). P_{lethal} was related to $P_{88,stem}$, SSM_{stem} and $SegP_{50}$ (Fig. 2b, Fig. S3). The interspecific variation in $P_{88,stem}$ encompassed the range of P_{lethal}, which corresponded to high values of $PLC_{leth,leaf}$ for all species ($\geq$ 96%) and a broader variation in $PLC_{leth,stem}$ (80-100%) for an average of 88 ± 2 % (Fig. 2b; Table S2). In well-watered plants, species with larger LS had higher $g_{s,max}$, higher values of P_{md}-P_{tlp}, less negative values of $P_{50,stem}$ and narrower SSM_{stem} (Fig. S3, S4).

NSC storage and use

After a severe drought, strong interspecific differences were observed regarding NSC storage and use, as revealed by the significant interaction between '*Species'* and '*Treatment'* for both starch and SS (Fig. 3). Whole plant starch concentrations were lower in all species, but this decrease was significant in nine out of 12 species (Fig. 3a) with a similar pattern across organs (Fig. S5a,b,c). Conversely, whole plant SS concentrations showed a general tendency towards a maintenance or a net accumulation (Fig. 3b), with contrasting patterns across organs (see '*Treatment'* effect in Fig. S5d,e,f). During the imposed drought, whole plant SS concentrations declined significantly in only one species, *S. pruriens*, to a mean concentration of 0.84 % DM, due to strong declines in all organs (Fig. 3; Fig. S5d,e,f). SS concentrations declined in some organs of some other species, yet not causing significant declines in

whole plant concentrations (i.e. in leaves of *D. guianensis* and in leaves and the stem of *H. utilis*). The response of NSC storage and use was not related to any hydraulic trait (Fig. S3).

Physiological processes leading to drought-induced mortality

After the imposed drought and irrespective of the strong interspecific differences in leaf starch and SS concentrations, all species had extremely high values of $PLC_{SW,leaf}$ (Fig. 4). Although starch concentrations were almost depleted in half of the investigated species, severe SS depletion occurred in only one species, *S. pruriens*. Similarly, stems of severely wilted plants exhibited high values of $PLC_{SW,stem}$, with much broader cross species differences than for leaves. If some species showed a strong depletion in starch concentrations (Fig. 3a), none showed a near-complete depletion in SS concentrations (Fig. 3b). Unfortunately, we could estimate $PLC_{SW,stem}$ for *S. pruri*ens, which showed a strong depletion in SS concentrations. In leaves and stems, PLC levels were not related to percent deviation in NSC concentrations (Fig. 4) nor to the amount of NSC used during drought (Fig. S3).

Relative importance of traits determining time to stem hydraulic failure – Sureau model

Time to stem hydraulic failure (THF) varied from 92 to 229 days across species (Table 2). THF was negatively related to g_{min} (Fig. 5), such that species with lower residual conductance exhibited greater drought survival. Variation in THF was not related to any other traits related to hydraulic strategies, nor to the variation in SS or starch concentrations during drought (Fig. 5; Fig. 6; Fig. S3; Fig. S7). The sensitivity analysis showed that THF was very sensitive to changes in g_{bark}, as shown by the high values of Sobol's total order indices (21-83 %; Fig. 7), followed by $P_{50,leaf}$ and $P_{50,stem}$ (3-41 %). The influence of changes in g_{min} and P_{tlp} were almost negligible (0-5 %). The relative importance of each trait depended on specie's hydraulic strategy: species with low values of g_{bark} such as *H. utilis* and *J. copaia* showed the highest values of the sensitivity indices for $P_{50,leaf}$ and $P_{50,stem}$.

DISCUSSION

The results obtained in the present study provide new insights into the adaptive strategies to drought of rainforest tree species. More specifically, we showed that the studied species had contrasting hydraulic strategies and that some hydraulic traits vary in a coordinated fashion. Despite these differences, our results suggest that hydraulic failure is a major cause of drought-induced mortality, but that carbon starvation may be more common than previously thought. We did not find evidence that the ability of these species to convert stored starch into SS delayed time to hydraulic failure. We however show that the interspecific variability in residual water losses may have strong implications for survival under drought conditions.

Contrasting drought-response strategies

Our study on potted saplings revealed contrasting hydraulic strategies among the 12 studied tropical rainforest tree species (Fig. 1). We observed key trade-offs between relatively dehydration-tolerant and relatively dehydration-avoidant strategies. More dehydration-tolerant strategies were characterized by more negative values of P_{lethal} and $P_{50,stem}$ as well as higher values of SSM_{stem} and of Seg_{P50}. Yet, five species (*E. coriacea*, *E. falcata*, *E grandiflora*, *P. officinalis*, *V. americana*) had similar values of P_{lethal} despite strongly contrasting values of $P_{88,stem}$ (Fig. 2b), which hints that a diversity of strategies may allow to withstand very negative water potentials. Species with more dehydration-avoidant strategies were characterized by lower values of g_{min}, which may allow them to minimize water losses and subsequent decreases in water potential, potentially compensating for their lower tolerance to dehydration (Fig. 2a).

Independently, $P_{50,leaf}$, SSM_{leaf} and A_l:A_s determined an orthogonal dimension of hydraulic strategies to the dehydration tolerance-avoidance dimension (Fig. 1). Less negative values of $P_{50,leaf}$ and therefore lower values of SSM_{leaf} were associated with higher values of SSM_{stem} and $SegP_{50}$, meaning that sacrificing leaves favors stem hydraulic safety (Fig. 2cd). Powers *et al.* (2020) showed that tropical tree species with larger SSM_{leaf} better survived during an extreme drought event. However, they did not investigate the prevalence of vulnerability segmentation; we may suspect that the result they obtained could simply emerge from a correlation between $P_{50,leaf}$ and $P_{50,stem}$, which has already been observed for tropical canopy trees (Levionnois *et al.,* 2020). This would unveil the stronger importance of SSM_{stem} than of SSM_{leaf} for survival. The existence of a vulnerability segmentation pattern may also explain why saplings of tropical rainforest species do not suffer from mortality when showing very high levels of leaf xylem embolism (Manzi *et al.,* 2022), as indicated by values of $PLC_{leth,leaf}$ exceeding 96% in all of the studied species (Table S2). For stem embolism tolerance, we

found that the $PLC_{leth,stem}$ threshold was on average of 88% across the 12 tropical rainforest species we studied, which is exactly the mean value reported for temperate species by Urli *et al.* (2013). Contrary to leaves, we observed that $PLC_{leth,stem}$ varied strongly across species, in part because of vulnerability segmentation. All species were able to withstand up to ~80% of stem xylem embolism yet some appeared to be extremely tolerant (Fig. 2b; Table S2), in line with previous observations on temperate and subtropical species (Brodribb *et al.,* 2010; Urli *et al.,* 2013; Li *et al.,* 2016; Adams *et al.,* 2017; Hammond *et al.,* 2019; Shao *et al.,* 2022). In our study, $PLC_{leth,stem}$ was not related to any of the measured traits, which means that other processes than those at play during dehydration define embolism tolerance and the eventual recovery from high levels of xylem embolism. Indeed, the recovery of hydraulic conductivity following severe damage to perennial organs may be linked to specie's ability to maintain cell vitality in both primary and secondary meristematic tissues such as undifferentiated apical cells and cambium, which determines the growth of new leaves or layers of xylem and phloem, respectively (Mantova *et al.,* 2021; Gauthey *et al.,* 2022, Mantova *et al.,* 2022).

Stomatal regulation estimated by leaf turgor loss point (P_{tlp}), and leaf size (LS) represented other dimensions of plant hydraulic strategies. The uncoupling of P_{tlp} with decreasing vulnerability of leaf and stem xylem to embolism further supports that early stomatal regulation may allow the avoidance of hydraulic dysfunction as a result of selective pressures favoring drought-survival (Martin-StPaul *et al.,* 2017; Ziegler *et al.,* 2019; Creek *et al.,* 2020).

Species with larger leaves had higher values of $g_{s,max}$, which may be permitted by wider xylem vessels (Sack *et al.,* 2012; Levionnois *et al.,* 2021b), and maintained greater stomatal opening at midday, according to higher values of the difference between P_{md} and P_{tlp} (Fig. S1). This may allow enhanced transpirational leaf cooling, limiting damage to the photosynthetic apparatus caused by high leaf temperatures (Michaeletz *et al.,* 2016). The growth of tropical rainforest species with larger leaves may yet be more sensitive to drought, which could hinder their competitive ability in drier habitats (Gaviria *et al.,* 2017; Levionnois, 2019). We also found that species with larger leaves had less negative values of $P_{50,stem}$ and narrower SSM_{stem}. This may explain why during heatwaves, they have been shown to be more prone to increased crown dieback because of their lower ability to limit water losses, precipitating the speed at which they reach thresholds of hydraulic dysfunction (Marchin *et al.,* 2021). Our results thus support that leaf size may also be a critical component of plant adaptive strategies to drought with larger leaves being disadvantaged.

Pervasive hydraulic failure despite strong depletion in stored NSC

During the severe drought period, most species (11 out of 12) were able to use and convert starch into SS (Fig. 3; Fig. S5). This result was surprising and contradicts previous drought studies (Hartmann *et*

al., 2013ab; Adams *et al.,* 2017; Blackman *et al.,* 2019), notably on rainforest tree species (O'Brien *et al.,* 2014, 2015) which consumed their SS with little or no depletion in starch concentrations. Our observations rather indicate that the studied species could plastically increase SS levels, through an active increase in the rate of conversion of starch to SS, and/or through a passive accumulation due to sink limitations and preferential accumulation of SS (Körner, 2015). This suggests that a strategy enabling the maintenance of osmoregulation through decreased osmotic potential may be common across Neotropical tree saplings, consistent with a recent meta-analysis (He *et al.,* 2020). In the studied species, the process of carbon starvation therefore seems to be widespread and could contribute to a sustained avoidance of a hydraulic limitation to the use of stored NSCs (O'brien *et al.,* 2014; Hartmann & Trumbore, 2016). This points out to the high tolerance of NSC use to declining hydration among rainforest tree species, irrespectively of the diversity of drought-responses we observed.

Despite contrasting hydraulic strategies and the potential interaction between processes, all species seem to be more prone to leaf and stem hydraulic failure than to carbon starvation as a proximal cause of organ and whole-plant mortality (Fig. 4). Since we did not investigate root xylem vulnerability to embolism, and since it has been shown that some species exhibit vulnerability segmentation between these organs (Hukin *et al.,* 2005; Skelton *et al.,* 2017; Creek *et al.,* 2018; Losso *et al.,* 2019), we cannot conclude on below-ground physiological processes leading to mortality. However, the change in stem and root NSC concentrations followed similar trends, despite some species' specific differences (Fig. S5). We can therefore favor the hypothesis of root hydraulic failure over carbon starvation at the exception of *S. pruriens*, which could have succumbed to a combination of processes through a hydraulic limitation to the accessibility to use stored NSC (Sala *et al.,* 2010; Sevanto *et al.,* 2014; Sevanto, 2018). Indeed, even if starch concentrations remained relatively high, SS were almost depleted (Fig. 3).

In this study, we investigated the effects of a single drought. However, much less is known on the long-term effects of NSC depletion during repeated droughts, for instance how it interacts with plant defense against pathogens, which may weaken plants and eventually cause mortality (McDowell *et al.,* 2022), or how it influences post-drought recovery in growth (Gauthey *et al.,* 2022), hydric status and gas-exchange (Manzi *et al.,* 2022). Other current limitations are that the minimum thresholds of SS required for survival are unknown but may be extremely low yet above zero (Hartmann, 2015; Wiley *et al.,* 2017; Weber *et al.,* 2018;), and may vary with drought stress intensity (Sevanto *et al.,* 2014).

Survival to extreme drought depends on residual water conductance

There were marked differences in specie's time to stem hydraulic failure (THF), revealing that species with contrasting hydraulic strategies may not perform equally during drought (Fig. 5; Fig. 6; Fig. S7).

Among the studied traits, only variation in g_{min} translated into variation in THF, indicating that a water-saving, dehydration-avoidant strategy is the most effective way to delay hydraulic failure. This is in line with other studies suggesting that residual water losses are an important feature controlling drought-survival (Martin StPaul *et al.,* 2017; Duursma *et al.,* 2019; Machado *et al.,* 2020; Levionnois *et al.,* 2021a). Strikingly, the absence of a signal between traits related to xylem vulnerability to embolism and THF further questions on the actual paradigm placing vulnerability to embolism as the key feature for drought-survival (Delzon & Cochard 2014; Brodribb 2017). This view is legitimate since the water threshold for drought-induced mortality is linked to stem xylem vulnerability to embolism, as revealed by the positive relationship we found between $P_{88,stem}$ and P_{lethal} (Fig. 2b) and previous studies in other biomes (Urli *et al.,* 2013). Yet is seems like the rate at which plants will reach such thresholds may be disproportionally governed by residual conductance (Billon *et al.,* 2020). This was clearly the case for the species we studied, in light of the trade-off between g_{min} and $P_{50,stem}$, with the effect of g_{min} prevailing. Employing such a modeling approach by simulating plants of similar leaf area was convenient to study the sole effects of physiological traits on drought-survival. Future work should however seek to validate these results by measuring physiological traits on plants grown in the field, which may exhibit contrasting growth strategies and occur preferentially in habitats with contrasting light and water availability (Baraloto *et al.,* 2007; Allié *et al.,* 2015). Similarly, drought-survival in the field may be the result of numerous confounding effects such as evaporative demand, water availability, drought legacies, competition, pathogens or herbivory (McDowell *et al.,* 2022).

The sensitivity analysis we conducted on THF simulated intraspecific variation in the hydraulic traits incorporated in *SurEau*. It revealed that potential variation in g_{bark} would have a tremendous influence on species drought-survival (Fig. 7), suggesting that THF would be greatly enhanced in plants with lower values of g_{bark}. We however observed some interspecific differences in the sensitivity of THF which was related to species hydraulic strategies (Fig. 1). In species with low g_{bark}, THF would be equally enhanced by vulnerability segmentation through less negative values of $P_{50,leaf}$ and more negative values of $P_{50,stem}$ (Fig. 2c,d) than by decreasing g_{bark}. At the interspecific level, lower values of g_{min} were related to delayed THF (Fig. 5d) but intraspecific variation in g_{min} had nearly no influence on THF, contrary to that of g_{bark} (Fig. 7). This is because the vulnerability segmentation pattern was pervasive across species at high leaf xylem embolism levels, such that following a dramatic reduction in leaf area, water losses would be disproportionately driven by g_{bark}. This has in fact been observed for saplings of drought-deciduous species in seasonally dry tropical forests (Wolfe, 2020). The negative relationship we found between g_{min} and THF may thus be simply correlative due to the realistic assumption we made for our modeling exercise, that g_{bark} was related and equal to g_{min}, and may reflect the mechanistic linkage between g_{bark} and THF.

Tree communities in French Guiana regularly experience several months with low precipitation, with on average 22 ± 8 days without precipitation, and up to 61 days during the strongest intensity dry seasons (Svensk *et al.,* 2020). Results from simulations indicate that THF (92-229 days) exceeds this duration in all species. This supports recent findings demonstrating that the most abundant tree species in the Guiana Shield are well protected against drought-induced hydraulic failure (Ziegler *et al.,* 2019), although the frequency of strong intensity droughts is increasing in the Eastern Amazon (Duffy *et al.,* 2015). Considering the local variation in topography, water availability and the establishment of rooting in later stages of ontogeny remain additional challenges to address whether species growing in contrasting habitats will respond to future conditions (Fortunel *et al.,* 2020).

CONCLUSIONS

This study, combining experimental and modeling approaches, suggests that the variability in hydraulic strategies across the studied species may effect drought-survival with possible implications on the response of tree community composition at the sapling stage. Such changes in community composition have already been documented across Amazonia, but a mechanistic explanation was lacking (Esquivel-Muelbert *et al.,* 2019). Integrating these findings in plant economics theory (i.e. fast-slow spectrum and growth-mortality trade-offs) may also bring insight into future forest dynamics. Indeed, growth stimulation by rising CO_2 levels may in turn shorten trees' lifespan (Brienen *et al.,* 2020), which would disadvantage fast-growing species with high residual water losses, exacerbating floristic shifts.

ACKNOWLEDGMENTS

We thank colleagues from the technical team at EcoFoG for their precious help during the whole duration of the shadehouse experiment, notably Benoît Burban, Jocelyn Cazal, Jean-Yves Goret and Audin Patient. We would also like to thank Carole Antoine, Maëlle Cario, Bruno Clair, Elia Dardevet, Olivier Jean Leonce Manzi, Louis Milhe and Lynda Si Ouali for technical assistance. We thank the SILVATECH platform for hosting non-structural carbohydrate analyses (SILVATECH, INRAE, 2018. Structural and Functional Analysis of Tree and Wood Facility, doi: 10.15454/1.5572400113627854E12) from UMR 1434 SILVA, 1136 IAM, 1138 BEF and 4370 EA LERMAB at the INRAE Grand-Est Nancy research center and analysis. The SILVATECH facility is supported by the French National Research Agency through the Laboratory of Excellence ARBRE (ANR-11-LABX-0002-01). We thank Julien Ruffault for sharing his R code to perform Sobol's sensitivity analysis. This study was funded by an "Investissement d'Avenir" grant from the Agence Nationale de la Recherche (CEBA: ANR-10-LABX-0025; ARBRE, ANR-11-LABX- 0002-01). CZ received an assistantship from Pôle A2F, Université de Lorraine, France.

AUTHOR CONTRIBUTIONS

C.Z., S.C., D.B. and C.S. conceived and designed the study; C.Z., S.C., C.S. and J.Y.G. produced measurements during the shadehouse experiment; L.F., B.G. and P.M. carried-out non-structural carbohydrate analysis; C.Z. performed data analysis; H.C. performed *SurEau* model simulations. C.Z. wrote the manuscript; all authors discussed the results and contributed valuable comments to the manuscript.

DATA AVAILABILITY

All data corresponding to species' mean trait values are included in the manuscript. All raw data generated during the current study are not publicly available at the moment because the authors of the study wish to keep them for further analysis. They will then be made public on an online repository. In the meantime, they can nonetheless be made available by the corresponding author upon request.

COMPETING INTERESTS

The authors declare no competing interests.

546 **REFERENCES**

547 Adams, H. D., Zeppel, M. J. B., Anderegg, W. R. L., Hartmann, H., Landhausser, S. M., Tissue, D.
548 T., . . . McDowell, N. G. (2017). A multi-species synthesis of physiological mechanisms in
549 drought-induced tree mortality. *Nat Ecol Evol, 1*(9), 1285-1291. doi:10.1038/s41559-017-
550 0248-x

551 Allie, E., Pelissier, R., Engel, J., Petronelli, P., Freycon, V., Deblauwe, V., . . . Baraloto, C. (2015).
552 Pervasive Local-Scale Tree-Soil Habitat Association in a Tropical Forest Community. *PLoS*
553 *One, 10*(11), e0141488. doi:10.1371/journal.pone.0141488

554 Baraloto, C., Bonal, D., & Goldberg, D. E. (2006). Differential seedling growth response to soil
555 resource availability among nine neotropical tree species. Journal of Tropical Ecology, 22(5),
556 487-497. doi: 10.1017/S0266467406003439

557 Baraloto, C., Morneau, F., Bonal, D., Blanc, L., & Ferry, B. (2007). Seasonal Water Stress Tolerance
558 and Habitat Associations within Four Neotropical Tree Genera. Ecology, 88(2), 478-489. doi:
559 10.1890/0012-9658(2007)88[478:SWSTAH]2.0.CO;2

560 Bartlett, M. K., Scoffoni, C., Ardy, R., Zhang, Y., Sun, S., Cao, K., & Sack, L. (2012). Rapid
561 determination of comparative drought tolerance traits: using an osmometer to predict turgor
562 loss point. *Methods in Ecology and Evolution, 3*(5), 880-888. doi:10.1111/j.2041-
563 210X.2012.00230.x

564 Billon, L. M., Blackman, C. J., Cochard, H., Badel, E., Hitmi, A., Cartailler, J., . . . Torres-Ruiz, J. M.
565 (2020). The DroughtBox: A new tool for phenotyping residual branch conductance and its
566 temperature dependence during drought. *Plant Cell Environ, 43*(6), 1584-1594.
567 doi:10.1111/pce.13750

568 Blackman, C. J., Creek, D., Maier, C., Aspinwall, M. J., Drake, J. E., Pfautsch, S., . . . Choat, B.
569 (2019). Drought response strategies and hydraulic traits contribute to mechanistic
570 understanding of plant dry-down to hydraulic failure. *Tree Physiol, 39*(6), 910-924.
571 doi:10.1093/treephys/tpz016

572 Blackman, C. J., Li, X., Choat, B., Rymer, P. D., De Kauwe, M. G., Duursma, R. A., . . . Medlyn, B.
573 E. (2019). Desiccation time during drought is highly predictable across species of Eucalyptus
574 from contrasting climates. *New Phytol, 224*(2), 632-643. doi:10.1111/nph.16042

575 Bongers, F., Poorter, L., Van Rompaey, R., & Parren, M. (1999). Distribution of twelve moist forest
576 canopy tree species in Liberia and Cote d'Ivoire: response curves to a climatic gradient.
577 *Journal of Vegetation Science, 10*(3), 371-382. doi: 10.2307/3237066

Brienen, R. J. W., Caldwell, L., Duchesne, L., Voelker, S., Barichivich, J., Baliva, M., . . . Gloor, E. (2020). Forest carbon sink neutralized by pervasive growth-lifespan trade-offs. *Nat Commun, 11*(1), 4241. doi:10.1038/s41467-020-17966-z

Brodribb, T. J. (2017). Progressing from 'functional' to mechanistic traits. *New Phytol, 215*(1), 9-11. doi:10.1111/nph.14620

Brodribb, T. J., Bowman, D. J., Nichols, S., Delzon, S., & Burlett, R. (2010). Xylem function and growth rate interact to determine recovery rates after exposure to extreme water deficit. *New Phytol, 188*(2), 533-542. doi:10.1111/j.1469-8137.2010.03393.x

Brodribb, T. J., Carriqui, M., Delzon, S., & Lucani, C. (2017). Optical measurement of stem xylem vulnerability. *Plant Physiol, 174*(4), 2054-2061. doi: 10.1104/pp.17.00552

Brodribb, T. J., Powers, J., Cochard, H., & Choat, B. (2020). Hanging by a thread? Forests and drought. *Science, 368*(6488), 261-266. doi:10.1126/science.aat7631

Brodribb, T. J., Skelton, R. P., McAdam, S. A., Bienaime, D., Lucani, C. J., & Marmottant, P. (2016). Visual quantification of embolism reveals leaf vulnerability to hydraulic failure. *New Phytol, 209*(4), 1403-1409. doi:10.1111/nph.13846

Browne, L., Markesteijn, L., Engelbrecht, B. M., Jones, F. A., Lewis, O. T., Manzané-Pinzón, E., . . . Comita, L. S. (2021). Increased mortality of tropical tree seedlings during the extreme 2015–16 El Niño. *Global Change Biology, 27*(20), 5043-5053. doi: 10.1111/gcb.15809

Buckley, T. N. (2019). How do stomata respond to water status? *New Phytol, 224*(1), 21-36. doi:10.1111/nph.15899

Choat, B., Brodribb, T. J., Brodersen, C. R., Duursma, R. A., Lopez, R., & Medlyn, B. E. (2018). Triggers of tree mortality under drought. *Nature, 558*(7711), 531-539. doi:10.1038/s41586-018-0240-x

Cochard, H., Pimont, F., Ruffault, J., & Martin-StPaul, N. (2021). SurEau: a mechanistic model of plant water relations under extreme drought. *Annals of Forest Science, 78*(2), 1-23. doi: 10.1007/s13595-021-01067-y

Creek, D., Blackman, C. J., Brodribb, T. J., Choat, B., & Tissue, D. T. (2018). Coordination between leaf, stem, and root hydraulics and gas exchange in three arid-zone angiosperms during severe drought and recovery. *Plant Cell Environ, 41*(12), 2869-2881. doi:10.1111/pce.13418

Creek, D., Lamarque, L. J., Torres-Ruiz, J. M., Parise, C., Burlett, R., Tissue, D. T., & Delzon, S. (2020). Xylem embolism in leaves does not occur with open stomata: evidence from direct observations using the optical visualization technique. *J Exp Bot, 71*(3), 1151-1159. doi:10.1093/jxb/erz474

611 Delzon, S., & Cochard, H. (2014). Recent advances in tree hydraulics highlight the ecological
612 significance of the hydraulic safety margin. *New Phytol, 203*(2), 355-358.
613 doi:10.1111/nph.12798
614 Drake, J. E., Tjoelker, M. G., Varhammar, A., Medlyn, B. E., Reich, P. B., Leigh, A., . . . Barton, C.
615 V. M. (2018). Trees tolerate an extreme heatwave via sustained transpirational cooling and
616 increased leaf thermal tolerance. *Glob Chang Biol, 24*(6), 2390-2402. doi:10.1111/gcb.14037
617 Duffy, P. B., Brando, P., Asner, G. P., & Field, C. B. (2015). Projections of future meteorological
618 drought and wet periods in the Amazon. *Proceedings of the National Academy of Sciences,*
619 *112*(43), 13172-13177. doi:10.1073/pnas.1421010112
620 Duursma, R. A., Blackman, C. J., Lopez, R., Martin-StPaul, N. K., Cochard, H., & Medlyn, B. E.
621 (2019). On the minimum leaf conductance: its role in models of plant water use, and
622 ecological and environmental controls. *New Phytol, 221*(2), 693-705. doi:10.1111/nph.15395
623 Duursma, R. A., & Choat, B. (2017). fitplc: an R package to fit hydraulic vulnerability curves.
624 *Journal of Plant Hydraulics*. doi: 10.20870/jph.2017.e002
625 Engelbrecht, B. M., Tyree, M. T., & Kursar, T. A. (2007). Visual assessment of wilting as a measure
626 of leaf water potential and seedling drought survival. *Journal of Tropical Ecology*, 497-500.
627 doi: 10.1017/S026646740700421X
628 Esquivel-Muelbert, A., Baker, T. R., Dexter, K. G., Lewis, S. L., Brienen, R. J. W., Feldpausch, T. R.,
629 . . . Phillips, O. L. (2019). Compositional response of Amazon forests to climate change. *Glob*
630 *Chang Biol, 25*(1), 39-56. doi:10.1111/gcb.14413
631 Falster, D. (2006). User's guide to SMATR: standardised major axis tests and routines version 2.0,
632 copyright 2006. *http://www.bio.mq.edu.au/ecology/SMATR/*.
633 Fargeon, H., Aubry-Kientz, M., Brunaux, O., Descroix, L., Gaspard, R., Guitet, S., . . . Hérault, B.
634 (2016). Vulnerability of commercial tree species to water stress in logged forests of the
635 Guiana Shield. *Forests, 7*(12), 105. doi:10.3390/f7050105
636 Fortunel, C., Ruelle, J., Beauchene, J., Fine, P. V., & Baraloto, C. (2014). Wood specific gravity and
637 anatomy of branches and roots in 113 Amazonian rainforest tree species across environmental
638 gradients. *New Phytol, 202*(1), 79-94. doi:10.1111/nph.12632
639 Fortunel, C., Stahl, C., Heuret, P., Nicolini, E., & Baraloto, C. (2020). Disentangling the effects of
640 environment and ontogeny on tree functional dimensions for congeneric species in tropical
641 forests. *New Phytol, 226*(2), 385-395. doi:10.1111/nph.16393
642 Gauthey, A., Peters, J. M. R., Lopez, R., Carins-Murphy, M. R., Rodriguez-Dominguez, C. M.,
643 Tissue, D. T., . . . Choat, B. (2022). Mechanisms of xylem hydraulic recovery after drought in
644 Eucalyptus saligna. *Plant Cell Environ, 45*(4), 1216-1228. doi:10.1111/pce.14265

Gaviria, J., Turner, B. L., & Engelbrecht, B. M. (2017). Drivers of tree species distribution across a tropical rainfall gradient. *Ecosphere, 8*(2), e01712. doi: 10.1002/ecs2.1712

Hammond, W. M., Yu, K., Wilson, L. A., Will, R. E., Anderegg, W. R. L., & Adams, H. D. (2019). Dead or dying? Quantifying the point of no return from hydraulic failure in drought-induced tree mortality. *New Phytol, 223*(4), 1834-1843. doi:10.1111/nph.15922

Hartmann, H. (2015). Carbon starvation during drought-induced tree mortality–are we chasing a myth? Journal of Plant Hydraulics 2: e-0005. doi: 10.20870/jph.2015.e005

Hartmann, H., Bastos, A., Das, A. J., Esquivel-Muelbert, A., Hammond, W. M., Martínez-Vilalta, J., . . . Ruthrof, K. X. (2022). Climate Change Risks to Global Forest Health: Emergence of Unexpected Events of Elevated Tree Mortality Worldwide. *Annual review of plant biology, 73*. doi: 10.1146/annurev-arplant-102820-012804

Hartmann, H., & Trumbore, S. (2016). Understanding the roles of nonstructural carbohydrates in forest trees - from what we can measure to what we want to know. *New Phytol, 211*(2), 386-403. doi:10.1111/nph.13955

Hartmann, H., Ziegler, W., Kolle, O., & Trumbore, S. (2013). Thirst beats hunger - declining hydration during drought prevents carbon starvation in Norway spruce saplings. *New Phytol, 200*(2), 340-349. doi:10.1111/nph.12331

Hartmann, H., Ziegler, W., Trumbore, S., & Knapp, A. (2013). Lethal drought leads to reduction in nonstructural carbohydrates in Norway spruce tree roots but not in the canopy. *Functional Ecology, 27*(2), 413-427. doi:10.1111/1365-2435.12046

He, W., Liu, H., Qi, Y., Liu, F., & Zhu, X. (2020). Patterns in nonstructural carbohydrate contents at the tree organ level in response to drought duration. *Global Change Biology, 26*(6), 3627-3638. doi: 10.1111/gcb.15078

Hochberg, U., Rockwell, F. E., Holbrook, N. M., & Cochard, H. (2018). Iso/Anisohydry: A Plant-Environment Interaction Rather Than a Simple Hydraulic Trait. *Trends Plant Sci, 23*(2), 112-120. doi:10.1016/j.tplants.2017.11.002

Hukin, D., Cochard, H., Dreyer, E., Thiec, D. L., & Bogeat-Triboulot, M. (2005). Cavitation vulnerability in roots and shoots: does Populus euphratica Oliv., a poplar from arid areas of Central Asia, differ from other poplar species? *Journal of Experimental Botany, 56*(418), 2003-2010. doi: 10.1093/jxb/eri198

Huntingford, C., Zelazowski, P., Galbraith, D., Mercado, L. M., Sitch, S., Fisher, R., . . . Booth, B. B. (2013). Simulated resilience of tropical rainforests to CO2-induced climate change. *Nature Geoscience, 6*(4), 268-273. doi: 10.1038/ngeo1741

678 Körner, C. (2015). Paradigm shift in plant growth control. *Curr Opin Plant Biol, 25*, 107-114.
679 doi:10.1016/j.pbi.2015.05.003
680 Kursar, T. A., Engelbrecht, B. M. J., Burke, A., Tyree, M. T., El Omari, B., & Giraldo, J. P. (2009).
681 Tolerance to low leaf water status of tropical tree seedlings is related to drought performance
682 and distribution. *Functional Ecology, 23*(1), 93-102. doi:10.1111/j.1365-2435.2008.01483.x
683 Larter, M., Pfautsch, S., Domec, J. C., Trueba, S., Nagalingum, N., & Delzon, S. (2017). Aridity
684 drove the evolution of extreme embolism resistance and the radiation of conifer genus
685 Callitris. *New Phytol, 215*(1), 97-112. doi:10.1111/nph.14545
686 Levionnois, S., Ziegler, C., Heuret, P., Jansen, S., Stahl, C., Calvet, E., . . . Coste, S. (2021a). Is
687 vulnerability segmentation at the leaf-stem transition a drought resistance mechanism? A
688 theoretical test with a trait-based model for Neotropical canopy tree species. *Annals of Forest*
689 *Science, 78*(4), 1-16. doi: 10.1007/s13595-021-01094-9
690 Levionnois, S., Salmon, C., Alméras, T., Clair, B., Ziegler, C., Coste, S., . . . Heuret, P. (2021b).
691 Anatomies, vascular architectures, and mechanics underlying the leaf size-stem size spectrum
692 in 42 Neotropical tree species. *Journal of Experimental Botany, 72*(22), 7957-7969. doi:
693 10.1093/jxb/erab379
694 Levionnois, S., Ziegler, C., Jansen, S., Calvet, E., Coste, S., Stahl, C., . . . Heuret, P. (2020).
695 Vulnerability and hydraulic segmentations at the stem-leaf transition: coordination across
696 Neotropical trees. *New Phytol, 228*(2), 512-524. doi:10.1111/nph.16723
697 Li, S., Feifel, M., Karimi, Z., Schuldt, B., Choat, B., & Jansen, S. (2016). Leaf gas exchange
698 performance and the lethal water potential of five European species during drought. *Tree*
699 *Physiol, 36*(2), 179-192. doi:10.1093/treephys/tpv117
700 Li, X., Blackman, C. J., Peters, J. M. R., Choat, B., Rymer, P. D., Medlyn, B. E., . . . Oliveira, R.
701 (2019). More than iso/anisohydry: Hydroscapes integrate plant water use and drought
702 tolerance traits in 10 eucalypt species from contrasting climates. *Functional Ecology, 33*(6),
703 1035-1049. doi:10.1111/1365-2435.13320
704 López, R., Cano, F. J., Martin-StPaul, N. K., Cochard, H., & Choat, B. (2021). Coordination of stem
705 and leaf traits define different strategies to regulate water loss and tolerance ranges to aridity.
706 *New Phytologist, 230*(2), 497-509. doi: 10.1111/nph.17185
707 Loram-Lourenço, L., Farnese, F. S., Alves, R. D. F. B., Dario, B. M. M., Martins, A. C., Aun, M. A., .
708 . . Franco, A. C. (2022). Variations in bark structural properties affect both water loss and
709 carbon economics in neotropical savanna trees in the Cerrado region of Brazil. *Journal of*
710 *Ecology*. doi: 10.1111/1365-2745.13908

711 Losso, A., Bar, A., Damon, B., Dullin, C., Ganthaler, A., Petruzzellis, F., . . . Beikircher, B. (2019).
712 Insights from in vivo micro-CT analysis: testing the hydraulic vulnerability segmentation in
713 Acer pseudoplatanus and Fagus sylvatica seedlings. *New Phytol, 221*(4), 1831-1842.
714 doi:10.1111/nph.15549
715 Machado, R., Loram-Lourenco, L., Farnese, F. S., Alves, R., de Sousa, L. F., Silva, F. G., . . .
716 Menezes-Silva, P. E. (2020). Where do leaf water leaks come from? Trade-offs underlying the
717 variability in minimum conductance across tropical savanna species with contrasting growth
718 strategies. *New Phytol*. doi:10.1111/nph.16941
719 Mantova, M., Cochard, H., Burlett, R., Delzon, S., King, A., Rodriguez-Dominguez, C. M., . . .
720 Torres-Ruiz, J. M. (2022). On the path from xylem hydraulic failure to downstream cell
721 death. *New Phytologist*. doi: 10.1111/nph.18578
722 Mantova, M., Herbette, S., Cochard, H., & Torres-Ruiz, J. M. (2021). Hydraulic failure and tree
723 mortality: from correlation to causation. *Trends Plant Sci*. doi: 10.1016/j.tplants.2021.10.003
724 Manzi, O. J. L., Bellifa, M., Ziegler, C., Mihle, L., Levionnois, S., Burban, B., . . . Stahl, C. (2022).
725 Drought stress recovery of hydraulic and photochemical processes in Neotropical tree
726 saplings. *Tree Physiol, 42*(1), 114-129. doi:10.1093/treephys/tpab092
727 Marchin, R. M., Backes, D., Ossola, A., Leishman, M. R., Tjoelker, M. G., & Ellsworth, D. S.
728 (2022). Extreme heat increases stomatal conductance and drought-induced mortality risk in
729 vulnerable plant species. *Global Change Biology, 28*(3), 1133-1146. doi: 10.1111/gcb.15976
730 Maréchaux, I., Bartlett, M. K., Sack, L., Baraloto, C., Engel, J., Joetzjer, E., . . . Kitajima, K. (2015).
731 Drought tolerance as predicted by leaf water potential at turgor loss point varies strongly
732 across species within an Amazonian forest. *Functional Ecology, 29*(10), 1268-1277.
733 doi:10.1111/1365-2435.12452
734 Martin-StPaul, N., Delzon, S., & Cochard, H. (2017). Plant resistance to drought depends on timely
735 stomatal closure. *Ecol Lett, 20*(11), 1437-1447. doi:10.1111/ele.12851
736 McDowell, N., Pockman, W. T., Allen, C. D., Breshears, D. D., Cobb, N., Kolb, T., . . . Yepez, E. A.
737 (2008). Mechanisms of plant survival and mortality during drought: why do some plants
738 survive while others succumb to drought? *New Phytol, 178*(4), 719-739. doi:10.1111/j.1469-
739 8137.2008.02436.x
740 McDowell, N. G. (2011). Mechanisms linking drought, hydraulics, carbon metabolism, and
741 vegetation mortality. *Plant Physiol, 155*(3), 1051-1059. doi:10.1104/pp.110.170704
742 McDowell, N. G., Sapes, G., Pivovaroff, A., Adams, H. D., Allen, C. D., Anderegg, W. R., . . . Choat,
743 B. (2022). Mechanisms of woody-plant mortality under rising drought, CO2 and vapour

pressure deficit. *Nature Reviews Earth & Environment*, 1-15. doi: 10.1038/s43017-022-00272-1

Meinzer, F. C., Woodruff, D. R., Marias, D. E., Smith, D. D., McCulloh, K. A., Howard, A. R., & Magedman, A. L. (2016). Mapping 'hydroscapes' along the iso- to anisohydric continuum of stomatal regulation of plant water status. *Ecol Lett, 19*(11), 1343-1352. doi:10.1111/ele.12670

Michaletz, S. T., Weiser, M. D., McDowell, N. G., Zhou, J., Kaspari, M., Helliker, B. R., & Enquist, B. J. (2016). The energetic and carbon economic origins of leaf thermoregulation. *Nat Plants, 2*, 16129. doi:10.1038/nplants.2016.129

Mitchell, P. J., O'Grady, A. P., Tissue, D. T., White, D. A., Ottenschlaeger, M. L., & Pinkard, E. A. (2013). Drought response strategies define the relative contributions of hydraulic dysfunction and carbohydrate depletion during tree mortality. *New Phytol, 197*(3), 862-872. doi:10.1111/nph.12064

O'Brien, M. J., Burslem, D. F., Caduff, A., Tay, J., & Hector, A. (2015). Contrasting nonstructural carbohydrate dynamics of tropical tree seedlings under water deficit and variability. *New Phytol, 205*(3), 1083-1094. doi:10.1111/nph.13134

O'Brien, M. J., Leuzinger, S., Philipson, C. D., Tay, J., & Hector, A. (2014). Drought survival of tropical tree seedlings enhanced by non-structural carbohydrate levels. *Nature Climate Change, 4*(8), 710-714. doi:10.1038/nclimate2281

Oliveira, R. S., Costa, F. R. C., van Baalen, E., de Jonge, A., Bittencourt, P. R., Almanza, Y., . . . Poorter, L. (2019). Embolism resistance drives the distribution of Amazonian rainforest tree species along hydro-topographic gradients. *New Phytol, 221*(3), 1457-1465. doi:10.1111/nph.15463

Oliveira, R. S., Eller, C. B., Barros, F. d. V., Hirota, M., Brum, M., & Bittencourt, P. (2021). Linking plant hydraulics and the fast–slow continuum to understand resilience to drought in tropical ecosystems. *New Phytologist, 230*(3), 904-923. doi: 10.1111/nph.17266

Pammenter, N. W., & Vander Willigen, C. (1998). A mathematical and statistical analysis of the curves illustrating vulnerability of xylem to cavitation. *Tree Physiology, 18*(8-9), 589-593. doi:10.1093/treephys/18.8-9.589

Phillips, O. L., Aragao, L., Lewis, S. L., Fisher, J. B., Lloyd, J., Lopez-Gonzalez, G., . . . Torres-Lezama, A. (2009). Drought Sensitivity of the Amazon Rainforest. *Science, 323*(5919), 1344-1347. doi:10.1126/science.1164033

Phillips, O. L., van der Heijden, G., Lewis, S. L., Lopez-Gonzalez, G., Aragao, L. E., Lloyd, J., . . . Vilanova, E. (2010). Drought-mortality relationships for tropical forests. *New Phytol, 187*(3), 631-646. doi:10.1111/j.1469-8137.2010.03359.x

778 Pivovaroff, A. L., Pasquini, S. C., De Guzman, M. E., Alstad, K. P., Stemke, J. S., Santiago, L. S., &
779 Field, K. (2016). Multiple strategies for drought survival among woody plant species.
780 *Functional Ecology, 30*(4), 517-526. doi:10.1111/1365-2435.12518
781 Powers, J. S., Vargas, G. G., Brodribb, T. J., Schwartz, N. B., Perez-Aviles, D., Smith-Martin, C. M.,
782 . . . Medvigy, D. (2020). A catastrophic tropical drought kills hydraulically vulnerable tree
783 species. *Glob Chang Biol, 26*(5), 3122-3133. doi:10.1111/gcb.15037
784 Puy, A., Piano, S. L., Saltelli, A., & Levin, S. A. (2022). sensobol: An R package to compute
785 variance-based sensitivity indices. *Journal of Statistical Software, 102*, 1-37. doi:
786 10.48550/arXiv.2101.10103
787 Rodriguez-Dominguez, C. M., Buckley, T. N., Egea, G., de Cires, A., Hernandez-Santana, V.,
788 Martorell, S., & Diaz-Espejo, A. (2016). Most stomatal closure in woody species under
789 moderate drought can be explained by stomatal responses to leaf turgor. *Plant Cell Environ,*
790 *39*(9), 2014-2026. doi:10.1111/pce.12774
791 Rosner, S., & Morris, H. (2022). Breathing life into trees: the physiological and biomechanical
792 functions of lenticels. *IAWA Journal, 43*(3), 234-262. doi: 10.1163/22941932-bja10090
793 Sack, L., & Scoffoni, C. (2011). Minimum epidermal conductance (gmin, aka cuticular
794 conductance). *PrometheusWiki, 35*, 257-262.
795 Sala, A., Piper, F., & Hoch, G. (2010). Physiological mechanisms of drought-induced tree mortality
796 are far from being resolved. *New Phytol, 186*(2), 274-281. doi: 10.1111/j.1469-
797 8137.2009.03167.x
798 Sevanto, S. (2018). Drought impacts on phloem transport. *Curr Opin Plant Biol, 43*, 76-81.
799 doi:10.1016/j.pbi.2018.01.002
800 Sevanto, S., McDowell, N. G., Dickman, L. T., Pangle, R., & Pockman, W. T. (2014). How do trees
801 die? A test of the hydraulic failure and carbon starvation hypotheses. *Plant Cell Environ,*
802 *37*(1), 153-161. doi:10.1111/pce.12141
803 Shao, J., Zhou, X., Zhang, P., Zhai, D., Yuan, T., Li, Z., . . . McDowell, N. G. (2022). Embolism
804 resistance explains mortality and recovery of five subtropical evergreen broadleaf trees to
805 persistent drought. *Ecology*, e3877. doi: 10.1002/ecy.3877
806 Skelton, R. P., Brodribb, T. J., & Choat, B. (2017). Casting light on xylem vulnerability in an
807 herbaceous species reveals a lack of segmentation. *New Phytol, 214*(2), 561-569.
808 doi:10.1111/nph.14450
809 Slot, M., Nardwattanawong, T., Hernández, G. G., Bueno, A., Riederer, M., & Winter, K. (2021).
810 Large differences in leaf cuticle conductance and its temperature response among 24 tropical

811 tree species from across a rainfall gradient. *New Phytologist, 232*(4), 1618-1631. doi:
812 10.1111/nph.17626
813 Sobol, I. M. (2001). Global sensitivity indices for nonlinear mathematical models and their Monte
814 Carlo estimates. *Mathematics and computers in simulation, 55*(1-3), 271-280. doi:
815 10.1016/S0378-4754(00)00270-6
816 Sperry, J. S., & Tyree, M. T. (1988). Mechanism of water stress-induced xylem embolism. *Plant*
817 *Physiol, 88*(3), 581-587.
818 Svensk, M., Coste, S., Gerard, B., Gril, E., Julien, F., Maillard, P., . . . Leroy, C. (2020). Drought
819 effects on resource partition and conservation among leaf ontogenetic stages in epiphytic tank
820 bromeliads. *Physiol Plant*. doi:10.1111/ppl.13161
821 Taiz, L., & Zeiger, E. (2002). Photosynthesis: physiological and ecological considerations. *Plant*
822 *Physiol, 9*, 172-174.
823 Torres-Ruiz, J. M., Jansen, S., Choat, B., McElrone, A. J., Cochard, H., Brodribb, T. J., . . . Delzon,
824 S. (2015). Direct x-ray microtomography observation confirms the induction of embolism
825 upon xylem cutting under tension. *Plant Physiol, 167*(1), 40-43. doi:10.1104/pp.114.249706
826 Tyree, M. T., Engelbrecht, B. M., Vargas, G., & Kursar, T. A. (2003). Desiccation tolerance of five
827 tropical seedlings in panama. Relationship to a field assessment of drought performance.
828 *Plant Physiol, 132*(3), 1439-1447. doi:10.1104/pp.102.018937
829 Tyree, M. T., & Sperry, J. S. (1988). Do woody plants operate near the point of catastrophic xylem
830 dysfunction caused by dynamic water stress? : answers from a model. *Plant Physiol, 88*(3),
831 574-580. doi:10.1104/pp.88.3.574
832 Tyree, M. T., Vargas, G., Engelbrecht, B. M., & Kursar, T. A. (2002). Drought until death do us part:
833 a case study of the desiccation-tolerance of a tropical moist forest seedling-tree, Licania
834 platypus (Hemsl.) Fritsch. *Journal of Experimental Botany, 53*(378), 2239-2247. doi:
835 10.1093/jxb/erf078
836 Urli, M., Porte, A. J., Cochard, H., Guengant, Y., Burlett, R., & Delzon, S. (2013). Xylem embolism
837 threshold for catastrophic hydraulic failure in angiosperm trees. *Tree Physiol, 33*(7), 672-683.
838 doi:10.1093/treephys/tpt030
839 Van Handel, E. (1965). Estimation of glycogen in small amounts of tissue. *Analytical biochemistry,*
840 *11*(2), 256-265. doi: 10.1016/0003-2697(65)90013-8
841 Volaire, F. (2018). A unified framework of plant adaptive strategies to drought: Crossing scales and
842 disciplines. *Glob Chang Biol, 24*(7), 2929-2938. doi:10.1111/gcb.14062

Warton, D. I., Duursma, R. A., Falster, D. S., & Taskinen, S. (2012). smatr 3-an R package for estimation and inference about allometric lines. *Methods in Ecology and Evolution, 3*(2), 257-259. doi: 10.1111/j.2041-210X.2011.00153.x

Weber, R., Schwendener, A., Schmid, S., Lambert, S., Wiley, E., Landhausser, S. M., . . . Hoch, G. (2018). Living on next to nothing: tree seedlings can survive weeks with very low carbohydrate concentrations. *New Phytol, 218*(1), 107-118. doi:10.1111/nph.14987

Wiley, E., Hoch, G., & Landhäusser, S. M. (2017). Dying piece by piece: carbohydrate dynamics in aspen (Populus tremuloides) seedlings under severe carbon stress. *Journal of Experimental Botany, 68*(18), 5221-5232. doi: 10.1093/jxb/erx342

Wolfe, B. T. (2020). Bark water vapour conductance is associated with drought performance in tropical trees. *Biol Lett, 16*(8), 20200263. doi:10.1098/rsbl.2020.0263

Ziegler, C., Coste, S., Stahl, C., Delzon, S., Levionnois, S., Cazal, J., . . . Bonal, D. (2019). Large hydraulic safety margins protect Neotropical canopy rainforest tree species against hydraulic failure during drought. *Annals of Forest Science, 76*(4). doi:10.1007/s13595-019-0905-0

TABLES

Table 1: Summary of species full botanical name, family, abbreviation code and mean (± SE) basal diameter (mm) and stem height (cm) at the ons*et* of the experiment, as wel as relative growth rate in stem volume (RGR; cm^3 $year^{-1}$) for the 12 studied rainforest tree species. Each experimental cycle lasted 4-5 months (cycle 1, June 2017-October 2017; Cycle 2, March 2018-August 2018; Cycle 3, October 2018-March 2019; Table 1).

Species	**Family**	**Code**	**Cycle**	**Basal diameter (mm)**	**Height (cm)**	**RGR (cm^3 $year^{-1}$)**
Dicorynia guianensis Amshoff	Fabaceae	*Dg*	3	5.9 ± 0.2	35 ± 2	8.0 ± 0.5
Eschweilera coriacea (DC.) S.A. Mori	Lecythidaceae	*Ec*	3	7.8 ± 0.2	50 ± 3	4.2 ± 0.4
Eperua falcata Aubl.	Fabaceae	*Ef*	1	4.7 ± 0.1	51 ± 2	7.5 ± 0.4
Eperua grandiflora (Aubl.) Benth.	Fabaceae	*Eg*	1	6.9 ± 0.2	46 ± 2	4.6 ± 0.3
Heritiera utilis (Sprague) Sprague	Malvaceae	*Hu*	2	13.4 ± 0.4	92 ± 4	3.2 ± 0.4
Jacaranda copaia (Aubl.) D. Don	Bignoniaceae	*Jc*	2	13.6 ± 0.3	78 ± 2	2.3 ± 0.3
Pterocarpus officinalis Jacq.	Fabaceae	*Po*	1	6.6 ± 0.3	63 ± 3	6.0 ± 0.7
Recordoxylon speciosum (Benoist) Gazel ex Barneby	Fabaceae	*Rs*	3	7.1 ± 0.3	40 ± 2	3.8 ± 0.7
Sterculia pruriens (Aubl.) K. Schum	Sterculiaceae	*Sp*	3	10.8 ± 0.3	74 ± 2	6.1 ± 0.4
Sextonia rubra (Mez) van der Werff	Lauraceae	*Sr*	2	8.3 ± 0.3	48 ± 2	4.2 ± 0.5
Tachigali melinonii (Harms) Zarucchi & Herend.	Fabaceae	*Tm*	2	7.4 ± 0.2	78 ± 4	5.7 ± 0.5
Vouacapoua americana Aubl.	Fabaceae	*Va*	1	6.0 ± 0.2	30 ± 1	3.1 ± 0.4

Table 2: Mean values (± SE) of key hydraulic traits of saplings of 12 rainforest tree species. P_{tlp}, leaf turgor loss point; $P_{50,leaf}$ and $P_{50,stem}$, the water potential causing 50% loss in leaf or stem hydraulic conductivity, respectively; SSM_{leaf} and SSM_{stem}, the leaf or stem stomatal hydraulic safety margin, respectively; $SegP_{50}$, the index of vulnerability segmentation; g_{min}, the minimum leaf conductance; LS, leaf size; A_l:A_s, the leaf area to stem area ratio. SSM_{leaf} and SSM_{stem} were calculated using species mean trait values of P_{tlp}, $P_{50,leaf}$ and/or $P_{50,stem}$ and therefore don't present standard error of the mean. Species values of SegP50 corresponding to a vulnerability segmentation pattern were marked with a "$^+$". Some trait values were not available for some species and were marked with a "-". P-values of one-way ANOVA tests for species effect are shown when applicable.

Species	P_{tlp} (MPa)	$P_{50,leaf}$ (MPa)	$P_{50,stem}$ (MPa)	$P88_{,stem}$ (MPa)	P_{lethal} (MPa)	SSM_{leaf} (MPa)	SSM_{stem} (MPa)	$SegP_{50}$ (MPa)	g_{min} (mmol m^{-2} s^{-1})	LS (cm^2)	A_l:A_s (cm^2 cm^{-2})	THF (days)
Dg	-1.5 ± 0.0	-3.2 ± 0.7	-3.3 ± 0.4	-4.4 ± 0.6	-5.4 ± 0.2	1.6	1.8	0.2	2.0 ± 0.2	83 ± 8	7000 ± 331	92
Ec	-1.9 ± 0.0	-1.8 ± 0.2	-3.0 ± 0.2	-3.9 ± 0.1	-7.0 ± 0.4	-0.1	1.1	1.2^+	0.9 ± 0.1	113 ± 13	4527 ± 229	113
Ef	-1.8 ± 0.0	-2.5 ± 0.2	-4.2 ± 0.4	-6.9 ± 0.6	-6.8 ± 0.4	0.7	2.3	1.7^+	2.2 ± 0.2	57 ± 5	2506 ± 151	106
Eg	-1.9 ± 0.1	-1.7 ± 0.6	-4.9 ± 0.4	-6.8 ± 0.8	-7.0 ± 0.4	-0.2	2.9	2.6^+	2.1 ± 0.3	50 ± 4	2138 ± 246	95
Hu	-1.7 ± 0.0	-	-2.3 ± 0.2	-3.1 ± 0.4	-4.4 ± 0.3	-	0.6	-	0.4 ± 0.1	105 ± 5	4118 ± 261	229
Jc	-1.5 ± 0.0	-	-2.0 ± 0.3	-3.8 ± 0.8	-3.9 ± 0.3	-	0.5	-	0.5 ± 0.1	88 ± 8	3932 ± 243	182
Po	-1.5 ± 0.0	-1.3 ± 0.3	-3.9 ± 1.0	-6.5 ± 1.5	-6.8 ± 0.4	-0.3	2.3	2.6^+	1.9 ± 0.4	74 ± 9	1853 ± 182	149
Rs	-1.7 ± 0.0	-2.7 ± 1.0	-3.0 ± 0.5	-4.5 ± 0.7	-5.5 ± 0.3	1.0	1.3	0.3	1.2 ± 0.1	71 ± 7	9164 ± 954	179
Sp	-1.8 ± 0.0	-1.6 ± 0.3	-	-	-4.9 ± 0.3	-0.2	-	-	1.2 ± 0.1	143 ± 17	5091 ± 587	172
Sr	-1.8 ± 0.1	-2.4 ± 1.5	-2.3 ± 0.4	-3.7 ± 1.0	-5.0 ± 0.4	0.7	0.5	-0.2	1.5 ± 0.3	138 ± 15	4146 ± 324	114
Tm	-1.9 ± 0.1	-2.2 ± 0.2	-3.0 ± 0.5	-4.4 ± 0.4	-6.1 ± 0.4	0.3	1.1	0.8	1.4 ± 0.1	26 ± 2	13154 ± 644	168
Va	-2.2 ± 0.1	-3.0 ± 0.3	-4.2 ± 0.7	-6.8 ± 1.1	-6.8 ± 0.6	0.8	2.0	1.3^+	1.3 ± 0.1	39 ± 2	5646 ± 424	199
p	< 0.001	0.27	-	-	< 0.001	-	-	-	< 0.001	< 0.001	< 0.001	-

FIGURES

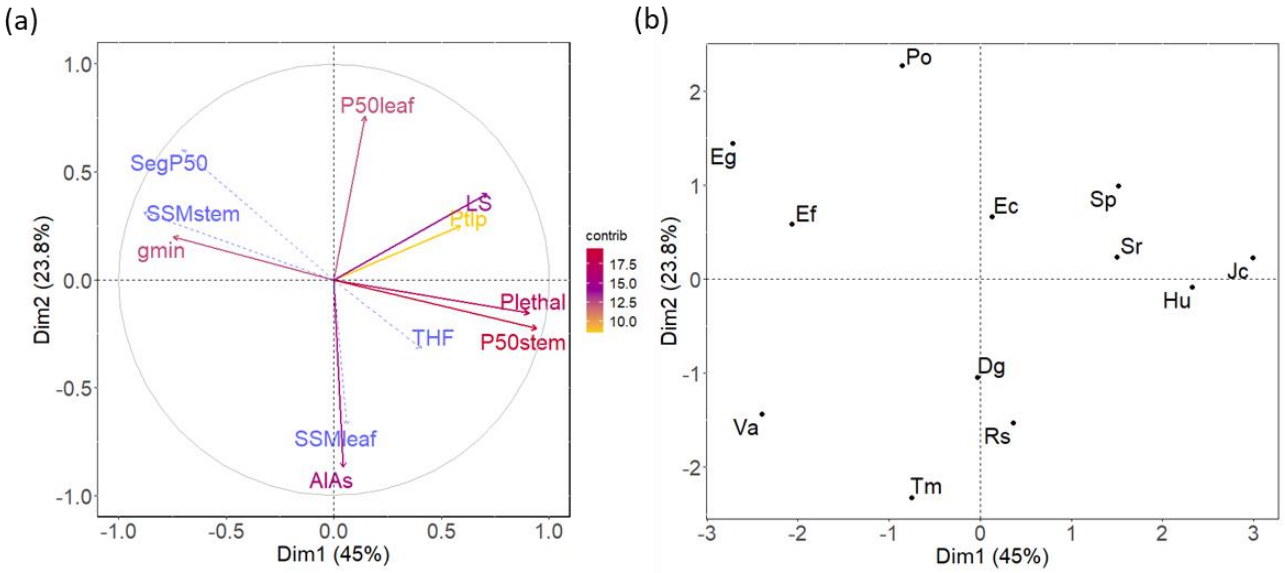

Figure 1: Bi-plot of principal component analysis (PCA) of the trade-offs between hydraulic traits defining species' drought-survival strategies for saplings of 12 rainforest tree species. Black points represent data for individual species. The percentages in the axis label indicate the variance explained by the axis. The relative contribution of each trait (%) is represented by a color gradient. Quantitative supplementary variables are represented by blue dashed lines. Traits: $P_{50,stem}$ and $P_{50,leaf}$, the water potentials associated with 50% loss of stem and leaf hydraulic conductance; P_{tlp}, the water potential at leaf turgor loss point; SSM_{stem} and SSM_{leaf}, the stem and leaf stomatal hydraulic safety margins; Seg_{P50}, the index of vulnerability segmentation; P_{lethal}, the water potential associated with 50% mortality; g_{min}, the minimum leaf conductance; LS, leaf size; A_l:A_s, the leaf to stem area ratio; THF, the modeled time to stem hydraulic failure.

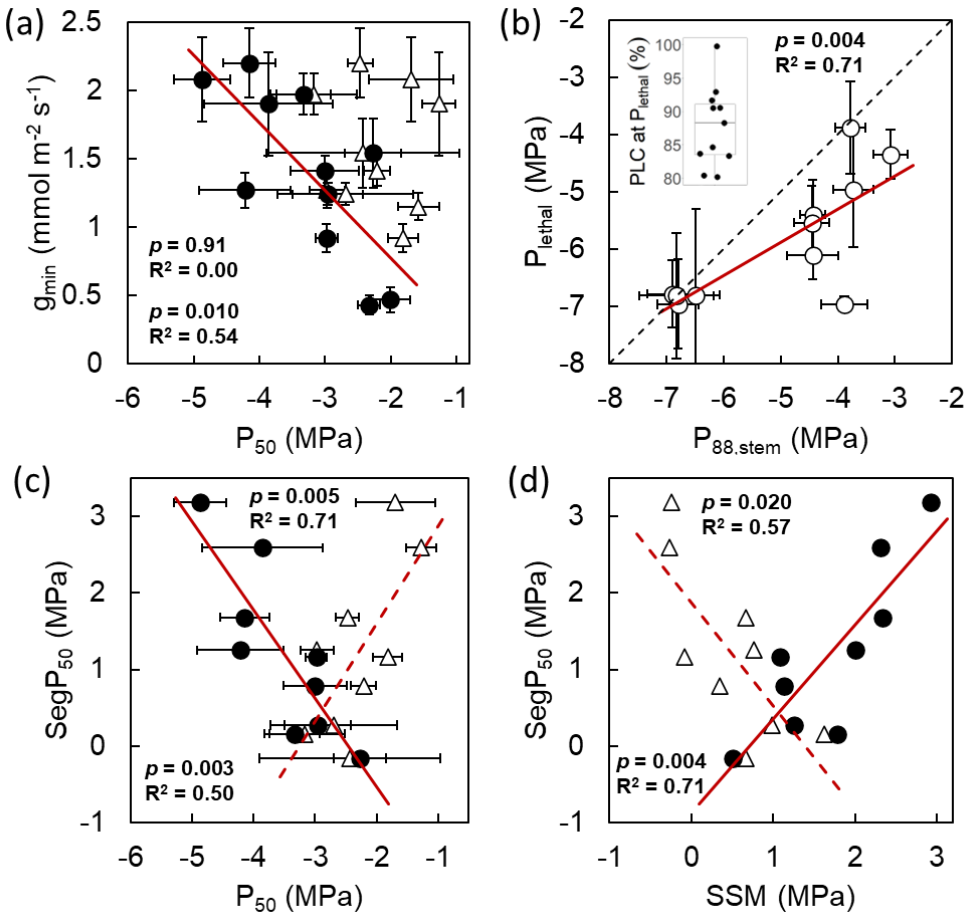

Figure 2: Correlations and trade-offs among hydraulic traits. Relationship between (a) the water potential associated with 50% loss of leaf or stem xylem hydraulic conductance ($P_{50,leaf}$, $P_{50,stem}$; MPa) and leaf minimum conductance (g_{min}; mmol m^{-2} s^{-1}); (b) the water potential associated with the mortality of 50% of saplings (P_{lethal}; MPa) and the water potential associated with 88% loss of stem xylem hydraulic conductance ($P_{88,stem}$; MPa). The boxplot in the insert shows the percent loss in stem xylem hydraulic conductance (PLC; %) once plants reach P_{lethal}. The box represents the 1st and 3rd quartiles, and error bars represent minimum and maximum values; (c) and (d) represents the variation of the index of vulnerability segmentation ($SegP_{50}$; MPa) as a function of $P_{50,leaf}$ and $P_{50,stem}$ as well as a function of the stomatal safety margin between turgor loss point and $P_{50,leaf}$ (SSM_{leaf}; MPa) or $P_{50,stem}$ (SSM_{stem}; MPa). Each point represents one species. Leaf and stem traits are represented by white triangles and black circles, respectively. Significant relationships are represented by bold solid (stems) and dashed lines (leaves). The thin dashed line represents the 1:1 line. Coefficients of determination (R^2) and significance levels (*p*) are shown. Error bars represent standard errors.

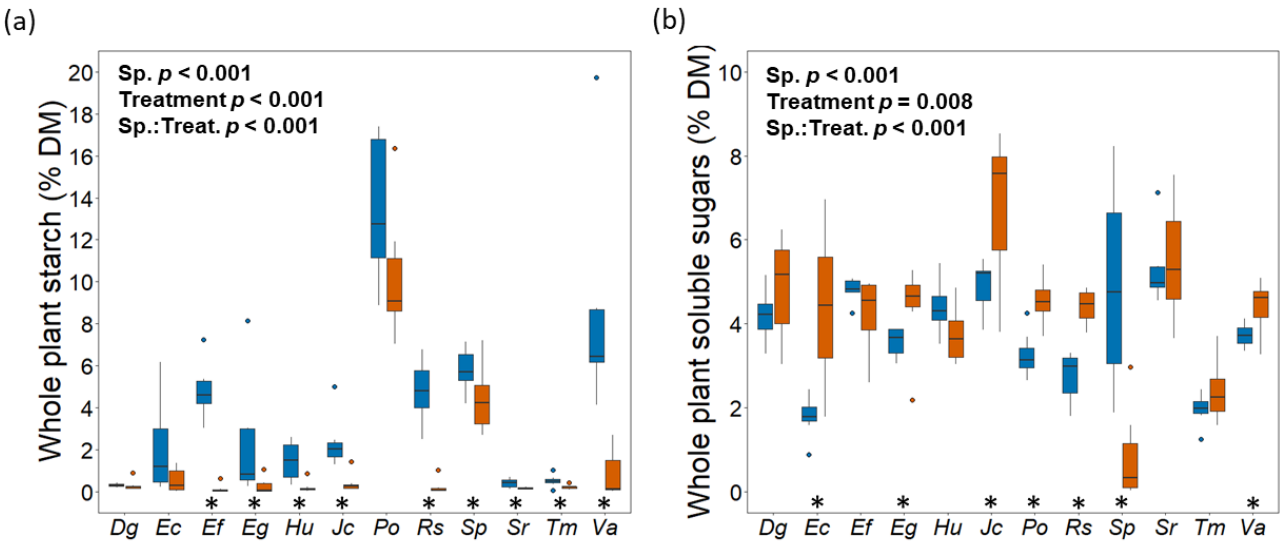

Figure 3: Response of carbon storage and use to a severe drought. Boxplots showing whole plant starch (a) and soluble sugar (b) concentrations in percent of dry matter (DM) of well-watered (blue) and droughted plants (red) for the 12 studied species. Boxes represent the median (horizontal line), 25th and 75th percentile; error bars show 95% confidence interval around the median; points represent significant outliers. Significant changes in soluble sugar or starch concentrations between treatments are denoted by an asterisk. Results of two-way ANOVAs with *Species* and *Treatments* as factors are shown.

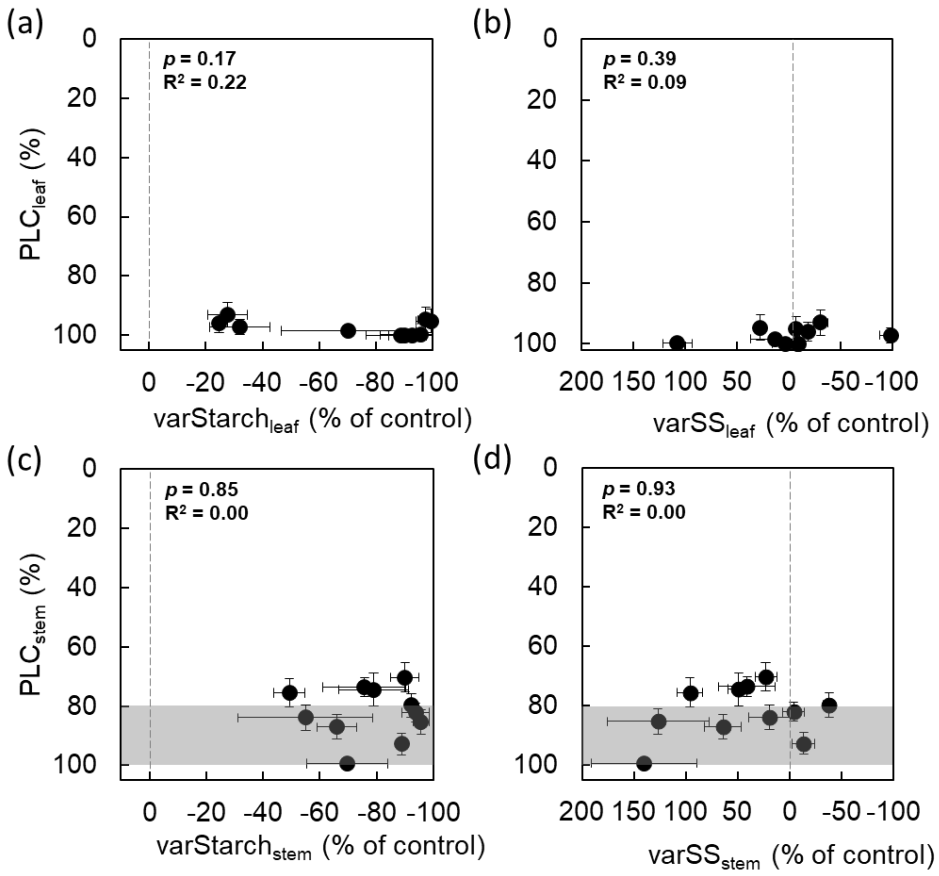

Figure 4: Leaf and stem physiological response associated with hydraulic failure and carbon starvation. Plots showing the relationships between the percent loss in leaf xylem hydraulic conductance (PLC_{leaf}; %) and the percent deviation in (a) leaf starch ($varStarch_{leaf}$; %) and (b) soluble sugar ($varSS_{leaf}$; %) concentrations for 10 of the studied species, as well as the relationships between the percent loss in stem xylem hydraulic conductance (PLC_{stem}; %) and the percent deviation in (c) stem starch ($varStarch_{stem}$; %) and (d) soluble sugar ($varSS_{stem}$; %) concentrations for 11 of the studied species in droughted and severely wilted plants compared to well-watered plants. Each point represents one species. Error bars represent standard errors. The thin vertical dashed line represents an absence of change in non-structural carbohydrate concentrations. The red shading represents the magnitude of PLC_{stem} associated with the water potential causing 50% mortality (P_{lethal}) across species according to the insert in Fig. 3.

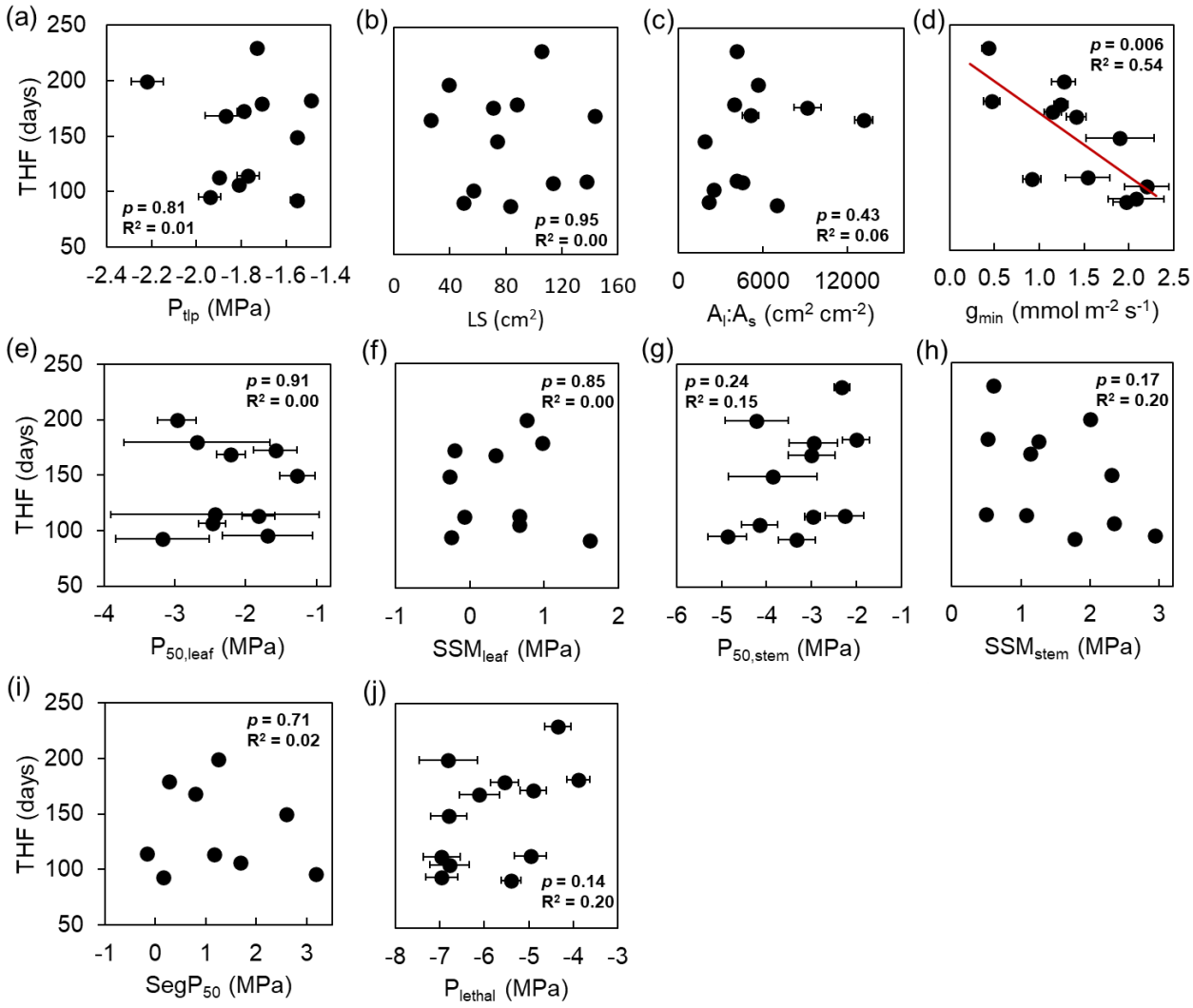

Figure 5: Correlations between traits determining hydraulic strategies and time to hydraulic failure (THF). Relationships between THF (days) and (a) leaf turgor loss point (Ptlp; MPa), (b) leaf size (LS; cm2), (c) leaf to stem area ratio (Al:As; cm2 cm2), (d) minimum leaf conductance (g_{min}; mmol m^{-2} s^{-1}), (e) leaf xylem vulnerability to embolism ($P_{50,leaf}$; MPa), (f) the leaf stomatal safety margin (SSM_{leaf}; MPa), (g) stem xylem vulnerability to embolism ($P_{50,stem}$; MPa), (h)) the stem stomatal safety margin (SSM_{stem}; MPa), (i) the index of vulnerability segmentation ($SegP_{50}$; MPa) and (j) the water potential associated with the mortality of 50% of saplings (P_{lethal}; MPa). Each point represents one species. Significant relationships are represented by bold solid lines. Coefficients of determination (R^2) and significance levels (*p*) are shown. Error bars represent standard errors.

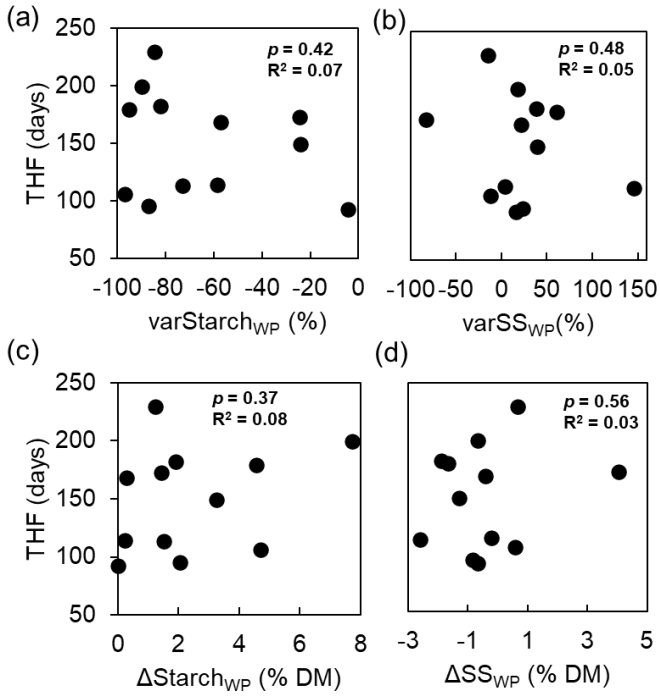

Figure 6: Correlations between traits determining whole plant non-structural carbohydrate use during drought and time to hydraulic failure (THF). Relationships between THF (days) and (a) the percent deviation in whole plant starch ($varStarch_{WP}$; %) and (b) soluble sugar ($varSS_{WP}$; %) concentrations between droughted and severely wilted plants compared to well-watered plants, as well as the difference in the amount, expressed as percent dry matter (% DM) of whole plant (c) starch ($\Delta Starch_{WP}$) and (d) soluble sugar (ΔSS_{WP}) in droughted compared to well-watered plants. Each point represents one species. Coefficients of determination (R^2) and significance levels (p) are shown. Error bars represent standard errors.

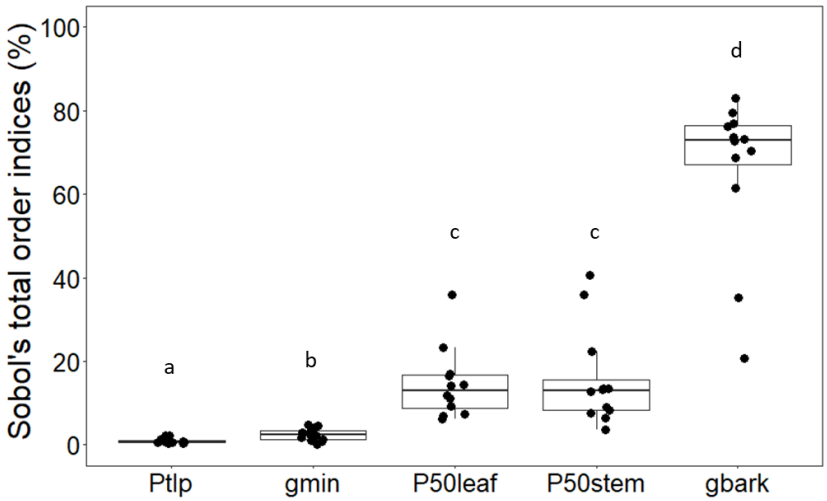

Figure 7: Global sensitivity analysis of plant time to hydraulic failure to variation in the main hydraulic traits in *SurEau*. Hydraulic traits varied from ± 20% around the mean measured value. Boxes represent the median (horizontal line), 25th and 75th percentile; error bars show 95% confidence interval around the median. Each point represents one species. Letters denote differences across traits.

SUPPLEMENTARY MATERIAL

Table S1: Percent change in soluble sugar and starch contents in leaves, stems and roots of droughted plants compared to well-watered plants Mean values (± SE) of the response of non-structural carbohydrate tissue concentrations, leaf and stem xylem hydraulic conductivity and species mortality rates of severely wilted saplings of 12 rainforest tree species. $varSS_{leaf}$, $varSS_{stem}$, $varSS_{root}$, $varStarch_{leaf}$, $varStarch_{stem}$, $varStarch_{root}$, $varSS_{WP}$ and $varStarch_{WP}$ the percent deviation of leaf, stem, root and whole plant (WP) soluble sugar (SS) or starch concentrations between droughted and well-watered plants; *p*-values of one-way ANOVA tests for species effect are shown.

Species	**$varSS_{WP}$ (%)**	**$varStarch_{WP}$ (%)**	**$varSS_{leaf}$ (%)**	**$varSS_{stem}$ (%)**	**$varSS_{root}$ (%)**	**$varStarch_{leaf}$ (%)**	**$varStarch_{stem}$ (%)**	**$varStarch_{root}$ (%)**
Dg	+16 ± 11	-4 ± 32	-31 ± 9	+64 ± 17	+90 ± 26	-28 ± 5	-66 ± 7	-51 ± 17
Ec	+146 ± 40	-73 ± 10	+107 ± 41	+140 ± 51	+201 ± 45	-96 ± 2	-70 ± 14	-60 ± 23
Ef	-12 ± 7	-97 ± 2	-9 ± 6	-4 ± 10	+2 ± 7	-93 ± 6	-94 ± 5	-98 ± 1
Eg	+23 ± 11	-87 ± 6	+3 ± 3	+49 ± 11	+30 ± 11	-89 ± 7	-79 ± 12	-91 ± 6
Hu	-15 ± 6	-85 ± 8	-57 ± 5	-38 ± 5	+47 ± 12	-88 ± 2	-92 ± 2	-78 ± 15
Jc	+38 ± 13	-82 ± 7	+42 ± 12	+41 ± 27	+52 ± 17	-94 ± 1	-76 ± 15	-89 ± 2
Po	+40 ± 6	-24 ± 9	-10 ± 5	+96 ± 12	+31 ± 9	-90 ± 2	-49 ± 5	-33 ± 12
Rs	+61 ± 6	-95 ± 3	+27 ± 20	+127 ± 49	+98 ± 27	-98 ± 0	-96 ± 3	-94 ± 3
Sp	-83 ± 8	-25 ± 10	-99 ± 1	-79 ± 11	-90 ± 4	-32 ± 4	-49 ± 11	+24 ± 17
Sr	+4 ± 10	-59 ± 5	-19 ± 8	-14 ± 11	+56 ± 17	-25 ± 12	-89 ± 2	-12 ± 14
Tm	+22 ± 14	-57 ± 8	+13 ± 11	+19 ± 20	+11 ± 13	-70 ± 6	-55 ± 24	-51 ± 14
Va	+18 ± 6	-90 ± 5	-7 ± 4	+23 ± 10	+49 ± 7	-100 ± 0	-90 ± 5	-84 ± 9
p	< 0.001	< 0.001	< 0.001	< 0.001	< 0.001	< 0.001	< 0.001	< 0.001

Table S2: Mean values (± SE) of the percentage loss in leaf and stem xylem hydraulic conductance of severely wilted plants ($PLC_{SW,leaf}$ and $PLC_{SW,stem}$, respectively; %) and at the water potential causing 50% mortality of saplings ($PLC_{leth,leaf}$ and $PLC_{leth,stem}$, respectively; %). P-values of one-way ANOVA tests for species effect are shown. (place next to

Species	**$PLC_{SW,leaf}$ (%)**	**$PLC_{leth,leaf}$ (%)**	**$PLC_{SW,stem}$ (%)**	**$PLC_{leth,stem}$ (%)**
Dg	93 ± 4	96 ± 2	87 ± 4	91 ± 3
Ec	100 ± 1	100 ± 0	99 ± 1	100 ± 0
Ef	100 ± 0	100 ± 0	82 ± 3	84 ± 3
Eg	100 ± 1	100 ± 0	74 ± 6	80 ± 5
Hu	-	-	80 ± 4	92 ± 2
Jc	-	-	74 ± 3	85 ± 2
Po	100 ± 0	100 ± 0	76 ± 5	83 ± 4
Rs	95 ± 4	96 ± 2	85 ± 4	88 ± 3
Sp	97 ± 2	99 ± 1	-	-
Sr	96 ± 3	97 ± 2	93 ± 4	90 ± 3
Tm	98 ± 2	100 ± 0	84 ± 4	93 ± 2
Va	95 ± 4	100 ± 0	70 ± 5	80 ± 5
p	0.028	0.09	< 0.001	< 0.001

Figure S1: Pictures of the leaves of the 12 studied species. All species except *E. coriacea*, *S. pruriens* and *S. rubra* have compound leaves.

Figure S2: Picture of the experimental setup in the shadehouse. For each species, plants were distributed homogenously according to stem height, basal diameter and maternal source. 24 saplings per species were well-watered three times a week to maintain high soil water availability while watering was withheld for 24 other plants to impose severe drought conditions. For each treatment, three blocks of 8 plants were randomly placed to account for potential differences in the local environment of the shadehouse, such that two blocks of the same species were not direct neighbors.

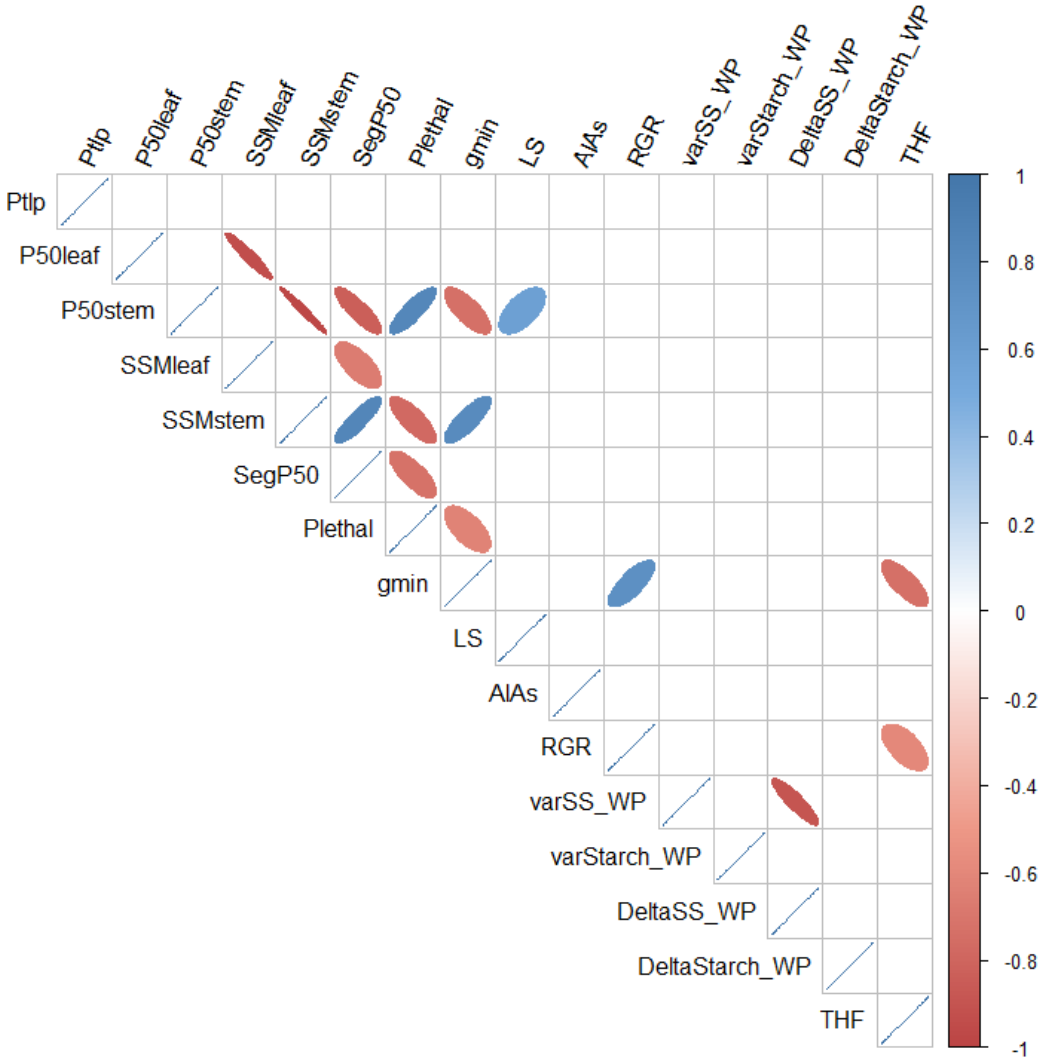

Figure S3: Pearson correlation matrix for pairwise relationships between traits determining hydraulic strategies, relative growth rate in stem volume of well-watered plants (RGR), traits relative to non-structural carbohydrate-use during drought and modeled time to hydraulic failure (THF). Significant relationships ($P < 0.05$) are displayed.

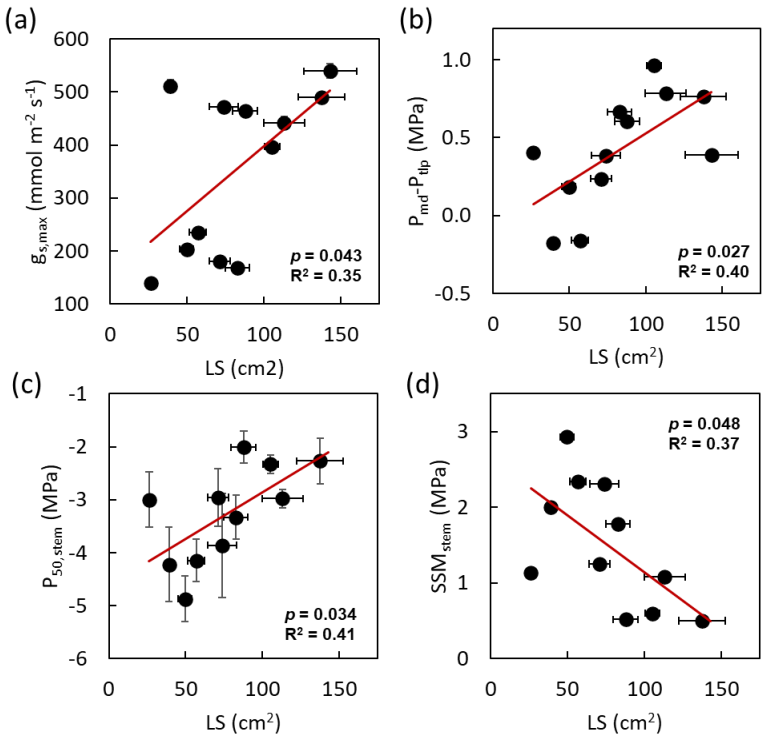

Figure S4 : Traits associated with leaf size. Relationship between leaf size (LS; cm^2) and (a) maximum stomatal conductance ($g_{s,max}$; mmol m^{-2} s^{-1}), (b) the difference between midday leaf water potential and turgor loss point (P_{md}-P_{tlp}; MPa), (c) the water potential associated with 50% loss of stem xylem hydraulic conductance ($P_{50,stem}$; MPa), (d) the stem stomatal safety margin between leaf turgor loss point and $P_{50,stem}$ (SSM_{stem}; MPa). Significant relationships are represented by bold solid lines. Coefficients of determination (R^2) and significance levels (*p*) are shown. Error bars represent standard errors.

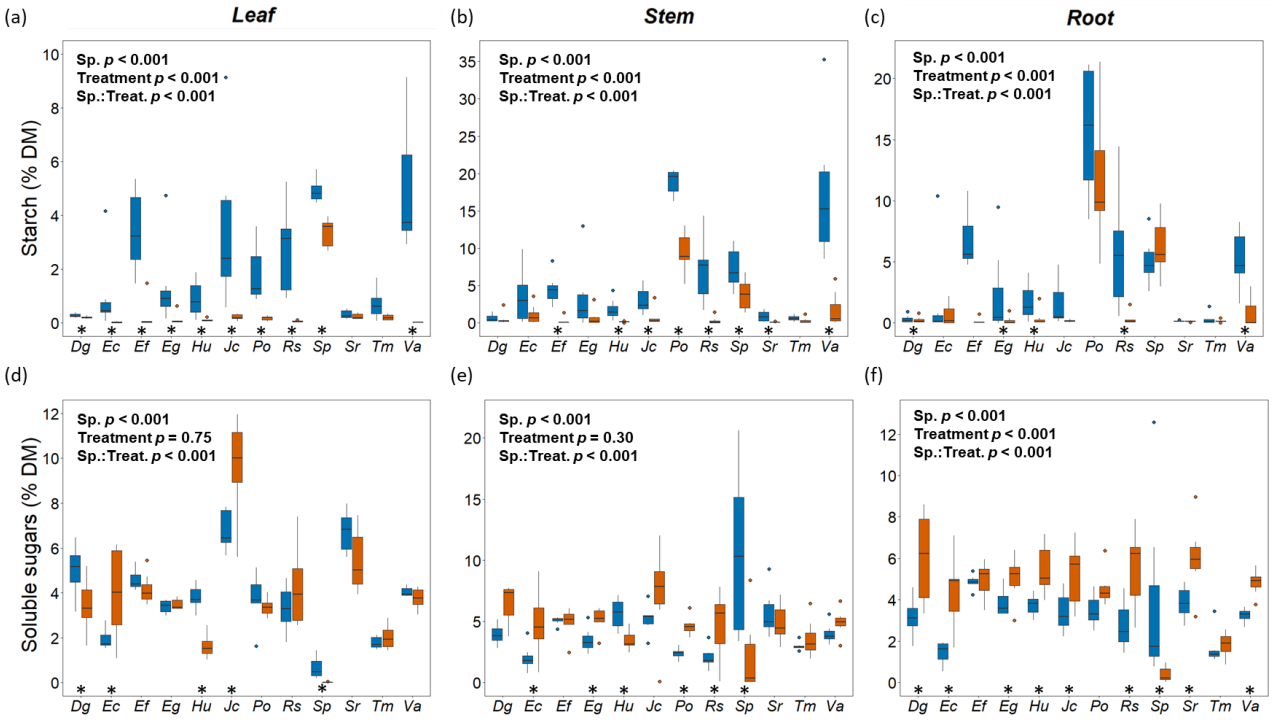

Figure S5: Response of carbon storage and use to a severe drought. Boxplots showing whole plant soluble sugar and starch concentrations in percent of dry matter (DM) in leaves (a, d), stems (b, e) and roots (c, f) of well-watered (blue) and droughted plants (red) for the 12 studied species. Significant changes in soluble sugar or starch concentrations between treatments are denoted by an asterisk. Boxes represent the median (horizontal line), 25th and 75th percentile; error bars show 95% confidence interval around the median; points represent significant outliers.

Extended description of Simulations with the SurEau model

To evaluate the contribution of the different physiological traits to the drought resistance of the studied species, we used the process-based *SurEau* model (Cochard *et al.,* 2021). *SurEau* simulates time to stem hydraulic failure (THF; days) by jointly considering stomatal and hydraulic traits, plant size, as well as climate and soil properties. The model assumes that THF depends on a two-stage process: the first stage comprises the time between the onset of drought and stomatal closure, depending on the transpiration rate and the water potential causing full stomatal closure. The second encompasses the time from stomatal closure to the critical water potential causing death, determined by minimum leaf and bark conductance, leaf and stem xylem vulnerability to embolism and plant water storage. The model was parameterized with species' trait data measured in this study.

We computed whole tree hydraulic conductance for each species knowing the midday leaf water potential and the transpiration of well-watered plants. The hydraulic conductances were then distributed in the different organs (leaf, branch, trunk, root) assuming that half of the resistance was located in the aerial organs and 80% of resistance in the symplasmic pathway. Stomatal closure occurred when the leaf water potential was equal to P_{tlp}. The formation and propagation of xylem embolism followed vulnerability curve parameters determined for leaves and stems. We assumed that the trunk and the roots had the same vulnerability than the branches. Area-based leaf residual water losses were estimated from g_{min} and leaf VPD values. Area-based bark residual conductance (g_{bark}) was estimated to be equal to g_{min} (Levionnois *et al.,* 2021a; Loram-Lourenço *et al.,* 2022). Internal water stores were estimated from stem volume based on interspecific variation of the leaf to stem area ratio (A_l:A_s). After stomatal closure, water losses were estimated from g_{min} and leaf area, and g_{bark} and bark area. The model parameters that were not measured were given realistic values according to the literature and considered constant across species. We simulated potted plants placed in the same growing conditions than for the experimental plants. To facilitate species comparison, we considered than the environmental conditions were constant in the greenhouse.

The simulation started with a soil water content set to its field capacity. The plant was then allowed to transpire which lowers the soil water content. We used pedotransfer functions (van Genuchten, 1980) to compute the soil water potential and the soil hydraulic conductance during dehydration. We used the van Genuchten parameter for a sandy-clay soil given by Bonan (2019). Area-based leaf water losses through transpiration were estimated using maximum stomatal conductance ($g_{s,max}$) and the VPD between the leaf and the ambient air. Leaf temperature was estimated by computing the leaf energy budget. We computed THF as the time between complete stomatal closure and the moment when the stem reaches 99 % loss of hydraulic conductivity, causing irreversible hydraulic damage and subsequent death by hydraulic failure. This threshold guarantees

that plant water pools were almost empty and that no other water reservoirs are available for the plant (Cochard *et al.,* 2021).

A first set of simulations was run using a mean estimated leaf area (A_l) per species. Species with larger A_l had shorter THF since A_l is a strong driver of water losses. Since it may be a confounding factor when predicting the kinetics of plant dehydration and desiccation (Lopez *et al.,* 2021), we ran a second set of simulations assuming species had a similar A_l, but specific values of A_l:A_s. Since we did not measure the water potential at stomatal closure directly from gas-exchange measurements, we also ran the model on the assumption that the point of stomatal closure corresponds to the formation of leaf xylem embolism, quantified as the water potential causing 12% of leaf xylem embolism ($P_{12,leaf}$). Values of simulated THF using either P_{tlp} or $P_{12,leaf}$ as an estimator of stomatal closure were strongly coordinated (Fig. S6). For data analysis, we further used THF simulated from P_{tlp} data. We then performed for each species a variance-based global sensitivity analysis to identify the hydraulic traits that influence THF. Variance-based approaches can measure sensitivity across the whole input space and quantify the effect of interactions that can be unnoticed on a local sensitivity analysis approach (i.e., when moving one parameter at a time). Here, we used the Sobol' sensitivity analysis method (Sobol, 2001) using the *sensobol* R package (Puy *et al.,* 2022), and reported 'Sobol's total order indices' that quantify the contribution of each parameter (i.e. hydraulic traits) to the variance of THF. For each species, we ran 10,000 simulations while allowing each parameter to vary randomly within a range of ±20% of the observed value.

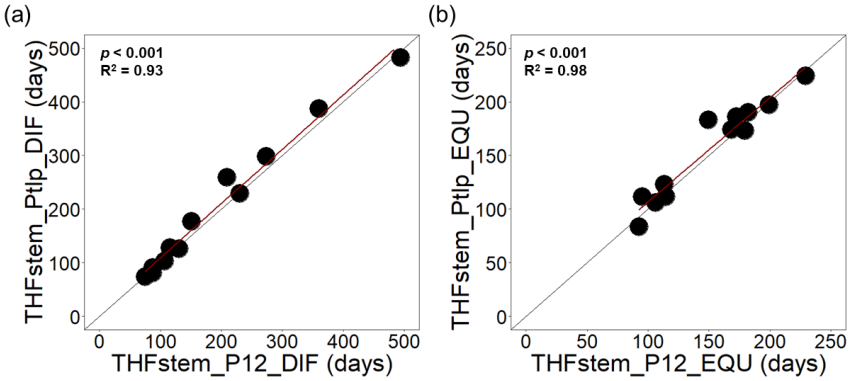

Figure S6: Comparison time to stem hydraulic failure (THF) between two different methods to estimate the water potential at stomatal closure (leaf turgor loss point, P_{tlp}, or the water potential inducing 12% of leaf xylem embolism, P12) during simulations with the *SurEau* model. Simulations considering species with similar (a) and different (b) total leaf area are shown. The red solid lines represent significant relationships. Coefficients of determination (R^2) and significance levels (*p*) are shown.

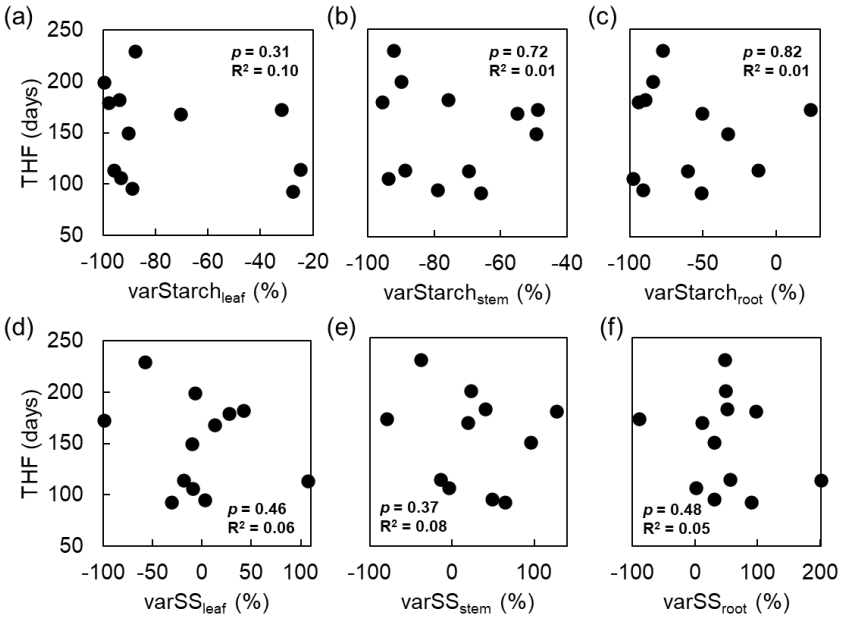

Figure S7: Correlations between traits determining organ-specific non-structural carbohydrate use during drought and time to hydraulic failure (THF). Relationships between THF (days) and the percent deviation in starch concentrations in (a) leaves, (b) stems and (c) roots ($varStarch_{leaf}$; $varStarch_{stem}$ and $varStarch_{root}$, respectively ;%), as well as the percent deviation in soluble sugar concentrations in (d) leaves, (e) stems and (f) roots ($varSS_{leaf}$; $varSS_{stem}$ and $varSS_{root}$, respectively ;%) of droughted and severely wilted plants compared to well-watered plants. Each point represents one species. Coefficients of determination (R^2) and significance levels (*p*) are shown. Error bars represent standard errors.

REFERENCES

Bonan, G. (2019). *Climate change and terrestrial ecosystem modeling*: Cambridge University Press. doi: 10.1017/9781107339217

Cochard, H., Pimont, F., Ruffault, J., & Martin-StPaul, N. (2021). SurEau: a mechanistic model of plant water relations under extreme drought. *Annals of Forest Science, 78*(2), 1-23. doi: 10.1007/s13595-021-01067-y

Levionnois, S., Ziegler, C., Heuret, P., Jansen, S., Stahl, C., Calvet, E., . . . Coste, S. (2021a). Is vulnerability segmentation at the leaf-stem transition a drought resistance mechanism? A theoretical test with a trait-based model for Neotropical canopy tree species. *Annals of Forest Science, 78*(4), 1-16. doi: 10.1007/s13595-021-01094-9

López, R., Cano, F. J., Martin-StPaul, N. K., Cochard, H., & Choat, B. (2021). Coordination of stem and leaf traits define different strategies to regulate water loss and tolerance ranges to aridity. *New Phytologist, 230*(2), 497-509. doi: 10.1111/nph.17185

Loram-Lourenço, L., Farnese, F. S., Alves, R. D. F. B., Dario, B. M. M., Martins, A. C., Aun, M. A., . . . Franco, A. C. (2022). Variations in bark structural properties affect both water loss and carbon economics in neotropical savanna trees in the Cerrado region of Brazil. *Journal of Ecology*. doi: 10.1111/1365-2745.13908

Puy, A., Piano, S. L., Saltelli, A., & Levin, S. A. (2022). sensobol: An R package to compute variance-based sensitivity indices. *Journal of Statistical Software, 102*, 1-37. doi: 10.48550/arXiv.2101.10103

Sobol, I. M. (2001). Global sensitivity indices for nonlinear mathematical models and their Monte Carlo estimates. *Mathematics and computers in simulation, 55*(1-3), 271-280. doi: 10.1016/S0378-4754(00)00270-6

Van Genuchten, M. T. (1980). A closed-form equation for predicting the hydraulic conductivity of unsaturated soils. *Soil science society of America journal, 44*(5), 892-898. Doi: 10.2136/sssaj1980.03615995004400050002x